# Chapter 3

# *MYR1* and *MYR2* are redundant genes that regulate lateral shoot outgrowth in Arabidopsis


## Abstract

Vascular tissues provide both the mechanical support to the plant body and the conducting cells for the transport of water, mineral solutes, hormones and other signaling molecules, amino acids, and sugars. To identify genes that may regulate vascular tissue-specific functions, we performed a genome-wide comparative analysis of phloem-cambium and xylem transcripts. In this chapter we focus on *MYR1* and *MYR2*, two G2-like transcription factors with phloem-specific expression. *MYR1* and *MYR2* are expressed as splice variants affecting the predicted coiled-coil region and/or the MYB-related domain, yielding three and six isoforms for *MYR1* and *MYR2*, respectively. Using a GAL4-based yeast assay, we demonstrated that both N- and C-terminal regions of the isoform MYR1-3 have transactivation activity. A GFP-based assay indicated that MYR1-3 is localized to the nucleus. T-DNA insertion lines for *MYR1* and *MYR2* were identified and both single (*myr1* and *myr2*) and double (*myr1myr2*) mutants were analyzed. Under continuous light, *myr1* plants did not appear to differ from wild type (wt) plants. However, *myr2* plants flowered early, with an average of 16.6 rosette leaves compared to 18.9 rosette leaves for wt plants. This early flowering phenotype was slightly more pronounced in *myr1myr2* plants where 15.3 rosette leaves were present at the time of flowering. *myr1myr2* plants exhibited additional differences in development compared to wt plants including elongated petioles, semi-erect leaf orientation and suppression of outgrowth of both secondary inflorescences and higher order branches on the primary inflorescence (i.e., increased apical dominance). These characteristics are reminiscent of *yucca*, a dominant Arabidopsis mutant with elevated levels of free auxin. In tryptophan analog (5-mT) feeding experiments, *myr1myr2* plants appeared to be the most resistant to 5-mT compared with wt and *myr1* or *myr2* plants, suggesting that MYR1 and MYR2 may be associated with tryptophan-dependent auxin biosynthesis. Interestingly, some transgenic plants overexpressing any one of the *MYR1* isoforms showed repression of lateral shoot outgrowth, similar to that observed in the

double mutant, suggesting that the regulation mediated by MYR1 and MYR2 may depend on formation of specific heterodimers consisting of isoforms of MYR1 and/or MYR2.

## Introduction

Branching plays an important role in the overall architecture of the mature plant. In higher plants, two developmental stages, the formation of axillary meristems and the outgrowth of axillary buds, are generally involved in the shoot branching process. Axillary shoot meristems may be derived directly from detached parts of the primary shoot apical meristems in some plants, e.g., tomato and potato, or they may develop from partially or fully differentiated cells that undergo dedifferentiation in the leaf axil in plants, such as Arabidopsis. After initiation, these axillary meristems may develop into elongated lateral shoot or initiate a few leaves and remain dormant, depending on the integration of genetic, developmental, and environmental information (for review, see Evans and Barton, 1997).

Several genes required for axillary shoot initiation have been identified, such as *Ls* (Schumacher et al., 1999) and *Bl* (Schmitz et al., 2002) in tomato; *LAS* (Greb et al., 2003) and *IFL1/REV* (Talbert et al., 1995; Zhong and Ye, 2001) in Arabidopsis; *MOC1* (Li et al., 2003), *OsTb1* (Takeda et al., 2003), and *LAX* (Komatsu et al., 2003) in rice; and *Tb1* (Doebley et al., 1997) and *BA1* (Gallavotti et al., 2004) in maize. Axillary meristem formation is almost completely blocked in the *ls* mutant during vegetative growth phase, whereas after the floral transition, the side shoots in the two leaf axils preceding an inflorescence develop normally. Mutations in the orthologous Arabidopsis gene, *LAS*, result in a phenotype similar to that observed in the *ls* mutant. The *moc1* mutant has almost no tillers (basal lateral shoots). Molecular analysis identified the *Ls* gene as a putative VHIID transcription factor of the GRAS family. *MOC1* is orthologous to *Ls*. Characterization of *Tb1* gene revealed that Tb1 is a member of the TCP family of DNA-binding transcriptional regulators. *OsTb1* appears to be regulated by *MOC1*. In contrast to the tomato *ls* mutant, the *lax* mutant has normal vegetative branching, but axillary meristem formation is severely suppressed during the reproductive phase. *LAX* encodes a basic helix-loop-helix transcription factor. More severe suppression was observed in the *ba1*, *bl*, and *rev* mutants. Lateral meristems in these mutants fail to initiate during both vegetative and reproductive growth phase, like *LAX*, *BA1* encodes a basic helix-loop-helix protein, whereas the *Bl* and *REV* genes encode a MYB transcription factor (the R2R3 class) (Stracke et al., 2001) and a homeodomain/leucine zipper transcription factor (the HD-ZIP-

START subgroup), respectively. These findings suggest that distinct classes of transcription factors are involved in controlling lateral meristem initiation.

Previous physiological observations through decapitation and/or hormone manipulation experiments, such as transgenic studies of plants with altered endogenous levels of auxin or cytokinin, suggest that the outgrowth of axillary buds is controlled by the interaction of auxin and cytokinin: auxin inhibits shoot branching, whereas cytokinin promotes it. Since auxin does not enter the bud, it does not suppress the outgrowth of axillary buds directly. In contrast to auxin, cytokinin can enter buds and promote their outgrowth (for review, see Napoli et al., 1999; Shimizu-Sato and Mori, 2001; Howell et al., 2003; Leyser, 2003; Ward and Leyser, 2004). A recent study showed that cytokinin biosynthesis is negatively mediated by auxin (Nordstrom et al., 2004).

Mutants with altered patterns of shoot branching were isolated from several plants species. These mutants can be grouped into three classes based on the pathways involved. In the first class, genes involved in auxin biosynthesis, transport, and signal transduction, or the integration of glucosinolate and auxin homeostasis are affected, including *YUCCA* (Zhao et al., 2001), *AXR1* (Leyser et al., 1993; Stirnberg et al., 1999; del pozo et al., 2002), *AXR3/IAA17* (Leyser et al., 1996; Ouellet et al., 2001), *IAA28* (Rogg et al., 2001), *BUS/SPS/CYP79F1* (Tantikanjana et al., 2001; Hansen et al., 2001; Chen et al., 2003; Tantikanjana et al., 2004). In the second class, a gene (*Sho*) involved in cytokinin biosynthesis is affected (Zubko et al., 2002). In the third class, genes involved in the production of a carotenoid-derived signal are affected, including *MAX1-MAX4* in Arabidopsis (Stirnberg et al., 2002; Sorefan et al., 2003; Booker et al., 2004; 2005), *RMS1-RMS6* in pea (Beveridge et al., 1996; 2000; Foo et al., 2001; 2005; Morris et al., 2001; Rameau et al., 2002), *DAD1-DAD3* in petunia (Napoli, 1996; Snowden and Napoli, 2003; Snowden et al., 2005), and D3 in rice (Ishikawa et al., 2005).

By performing a genome-wide comparative analysis of phloem-cambium and xylem transcripts using the 24KGeneChip, we identified several potential regulators of vascular differentiation and function, including 5 phloem-cambium-biased G2-like family members:

APL, MYR1, MYR2, At2g03500, and At3g12730 (Zhao et al., 2005). APL is required for phloem identity (Bonke et al., 2003). In this chapter we focus on *MYR1* and *MYR2*, and show that *myr1 myr2* double mutant plants exhibit suppression of lateral shoot outgrowth. Additionally, overexpression of each of three *MYR1* isoforms produced an apical dominance phenotype similar to that observed in the double mutant, suggesting that lateral shoot outgrowth mediated by MYR1 and MYR2 may depend on the formation of specific heterodimers consisting of isoforms of MYR1 and/or MYR2 and that correct dimerization may be disrupted in both loss- and gain-of-function plants.

## Materials and methods

### Phylogenetic analysis

Sequence alignments were produced using CLUSTALW 1.8 (http://clustalw.genome.jp) and the alignment was saved in PHYLIP format. Phylogenetic analysis was performed using PHYLIP-3.63 (http://evolution.genetics.washington.edu/phylip.html) as described (Brinkman and Leipe, 2001), and the tree (phylogram) was generated using TreeView 1.6.6 (http://taxonomy.zoology.gla.ac.uk/rod/treeview.html).

### Vector construction

#### pGEM-*MYR1p, -gMYR1, -cMYR1, -MYR1 3', -MYR2p, -gMYR2, -cMYR2,* and -*MYR2 3'*

The *MYR1* and *MYR2* putative promoters and 5' untranslated regions (termed as putative promoters in short), *MYR1p* and *MYR2p* (1.471- and 2.08-kb regions upstream from the MYR1 and MYR2 translation start, respectively), *MYR1* and *MYR2* genomic DNA, *gMYR1* and *gMYR2*, and their cDNA, *cMYR1* and *cMYR2*, and *MYR1* and *MYR2* 3' untranslated regions and terminal regions, *MYR1 3'* and *MYR2 3'* (1.405- and 1.522-kb regions downstream from the MYR1 and MYR2 translation stop, respectively) were amplified by PCR using genomic DNA or bark cDNA library (Zhao et al., 2000) as a template with following primers: 1) for *MYR1p*, an upstream *EcoR V* (underlined) linker primer 5'-GATATCAATTGCACATAGAGAAGCCA-3' and a downstream *BamH I* linker primer 5'-GGATCCAGTCTGTCTTCAAAATAAAAAGG-3'; 2) for *gMYR1* and *cMYR1*, an upstream *BamH I* linker primer 5'-GGATCCATGTATTACCACAACCAGCAC-3' and a downstream *EcoR V* linker primer 5'-GATATCTCAATTCCAGCTGAAACCATTT-3'; 3) for *MYR1* 3', an upstream *BamH I* (italic)/ *EcoR V* linker primer 5'-*GGATCC*GATATCGAAGAACAAATAAGCTTTAGAAG-3' and a downstream *Sma I* linker primer 5'-CCCGGGATTGGATCTTTTGTGGATTTG-3'; 4) for *MYR2p*, an upstream *Xba I* linker primer 5'-TCTAGAGCTTCGAAGCATCATTAG-3' and a downstream *BamH I* linker primer 5'-GGATCCAAAGTCTGTGCAACTGTAAGT-3'; 5) for *gMYR2* and *cMYR2*, an upstream *BamH I* linker primer 5'-GGATCCATGTATTACCAAAACCAGCAC-3' and a downstream *Sma I* linker primer 5'-CCCGGGAAACTCTCTTTTAACTTTTTGG-3'; 6) for *MYR2* 3', an upstream *BamH I*

(italic)/ *Swa I* linker primer 5'-*GGATCC*ATTTAAATCATTTCTGAGTTCACACAG-3' and a downstream *Sma I* linker primer 5'-CCCGGGAAGGTTGATGCGGTGAAGAA-3'. The PCR products were cloned into pGEM (pGEM was named for pGEM-T Easy Vector in short) (Promega, Madison, WI), thus generating pGEM-*MYR1p*, -*gMYR1*, -*cMYR1*, -*MYR1 3'*, -*MYR2p*, -*gMYR2*, -*cMYR2*, and -*MYR2 3'*, respectively.

***MYR1p-GUS, MYR2p-GUS, MYR1p-GFP, MYR1p-MYR1-3-GFP,* and *35S-MYR1-3-GFP***

A fragment containing *MYR1p* or *MYR2p* was excised from pGEM-*MYR1p* or -*MYR2p* (antisense orientation in pGEM) using *Spe I* /*BamH I* (the *Spe I* site is located on the vector) and inserted into the *Xba I*/*BamH I* site of mpBI121.3 (see the construction of mpBI121 in Appendix I), thereby producing mpBI121-*MYR1p-GUS* or mpBI121-*MYR2p-GUS*.

To place the *smGFP* coding sequence under control of *MYR1p*, A *BamH I*/*Sst I* fragment containing *smGFP* was shuttled from pGEM-*smGFP* (see the construction of *35S-GFP* in the Appendix I) to mpBI121-*MYR1p-GUS* using the same sets of restriction enzymes, thus replacing *GUS* with *GFP* and producing mpBI121-*MYR1p-GFP*.

To generate *MYR1p-MYR1-3-GFP* and *35S-MYR1-3-GFP*, the *MYR1-3* coding region (without the stop codon) was amplified from plasmid DNA pGEM-*MYR1-3* (with the stop codon) by PCR using an upstream *BamH I* linker primer 5'-GGATCCATGTATTACCACAACCAGCAC-3' and a downstream *EcoR V* linker primer GATATCATTCCAGCTGAAACCATTTAAATC-3'. The resulting PCR products were cloned into pGEM to produce pGEM-*MYR1-3* (without the stop codon). A fragment containing the *MYR1-3* (without the stop codon) was excised from pGEM-*MYR1-3* (without the stop codon) using *BamH I*/*EcoR V* and introduced into the *BamH I*/*Sma I* sites of mpBI121-*MYR1p-GFP* and mpBI121-*35S-GFP* (see the construction of *35S-GFP* in Appendix I) using the same sets of restriction enzymes, respectively.

***MYR1p-gMYR1, MYR1p-gMYR2, MYR2p-gMYR1,* and *MYR2p-gMYR2***

An *EcoR V*/*BamH I* fragment containing *MYR1p* was excised from pGEM-*MYR1p* (with an *EcoR V* site) and cloned into pGEM-*gMYR2* (sense orientation) digested with *Sma I/BamH I*, thus generating pGEM-*MYR1p* (antisense orientation and without an *EcoR V* site). A *Spe I*/*BamH I* fragment containing *MYR1p* or *MYR2p* was excised from pGEM-*MYR1p* (antisense orientation and without an *EcoR V* site) or -*MYR2p* (antisense orientation) and cloned into the *Spe I*/*BamH I* site of pGEM-*MYR1 3'* or -*MYR2 3'* (antisense orientation), thus generating pGEM-*MYR1p-MYR1 3'* and -*MYR2p-MYR2 3'*, respectively. A fragment containing *gMYR1* or *gMYR2* was excised from pGEM-*gMYR1* or -*gMYR2* using *BamH I*/ *EcoR V* or *BamH I*/ *Sma I* and introduced into pGEM-*MYR1p-MYR1 3'* and -*MYR2p-MYR2 3'* using *BamH I*/ *EcoR V* or *BamH I*/ *Swa I*, respectively, thus yielding pGEM-*MYR1p-gMYR1-MYR1 3'*, -*MYR1p-gMYR2-MYR1 3'*, -*MYR2p-gMYR1-MYR2 3'*, -*MYR2p-gMYR2-MYR2 3'*. Fragments containing *MYR1p-gMYR1-MYR1 3'*, *MYR1p-MYR1 3'*, *MYR2p-MYR2 3'*, *MYR2p-gMYR2-MYR2 3'* chimeric genes were excised from pGEM-*MYR1p-gMYR1-MYR1 3'*, -*MYR1p-MYR1 3'*, -*MYR2p-MYR2 3'*, -*MYR2p-gMYR2-MYR2 3'* using *Spe I*/ *Sma I* and inserted into the *Xba I*/*Sma I* site of mpFGC5941 (see the construction of mpFGC5941 in Appendix I), thus generating mpFGC5941-*MYR1p-gMYR1-MYR1 3'*, -*MYR1p-MYR1 3'*, -*MYR2p-MYR2 3'*, and -*MYR2p-gMYR2-MYR2 3'*. To generate mpFGC5941-*MYR1p-gMYR2-MYR1 3'* and -*MYR2p-gMYR1-MYR2 3'*, A fragment containing *gMYR2-MYR1 3'*or *gMYR1-MYR2 3'* was excised from pGEM-*MYR1p-gMYR2-MYR1 3'* or -*MYR2p-gMYR1-MYR2 3'* using *BamH I*/ *Sma I* and introduced into mpFGC5941-*MYR1p-MYR1 3'* and -*MYR2p-MYR2 3'* using the same sets of restriction enzymes, thus replacing *MYR1 3'* and *MYR2 3'* with *gMYR2-MYR1 3'* and *gMYR1-MYR2 3'*, respectively.

***35S-MYR1-1, -2, -3 and -MYR2-1.1, -2.1, -3.1***

To isolate *MYR1-1*, *MYR1-2*, and *MYR1-3*, plasmid DNA pGEM-*cMYR1* was digested by *EcoR I*/ *Sac I* (*Sac I* digests *MYR1-2* two times, *MYR1-1* and *MYR1-3* one time) to separate *MYR1-2* from *MYR1-1* and *MYR1-3*. *MYR1-1* could be separated from *MYR1-3* by digesting with *EcoR I*/*Rsa I* (*Rsa I* digests *MYR1-1* two times, *MYR1-3* one time). To isolate *MYR2-1.1*, *MYR2-2.1* and *MYR2-3.1*, plasmid DNA pGEM-*cMYR2* was digested with *EcoR I*/ *Rsa I* (*Rsa I* digests *MYR2-1.1* 5 times, *MYR2-2.1* and *MYR2-3.1* 4 times).

Fragments containing *MYR1-1, -2, -3* and *MYR2-1.1, -2.1, -3.1* were excised from pGEM-*MYR1-1, -2, -3* and -*MYR2-1.1, -2.1, -3.1* using *BamH I/ EcoR V* or *BamH I*/ *Sma I* and cloned into pFGC5941 using *BamH I/ Sma I*. The resulting plasmid DNA was digested with *Xho I/ BamH I*, blunted, and re-ligated, thus removing the CHSA intron between the *Xho I* and *BamH I* sites, thus yielding pFGC5941-*35S-MYR1-1, -2, -3* and pFGC5941-*35S-MYR2-1.1, -2.1, -3.1*, respectively.

**pGBKT7-*MYR1-3* and –*MYR1-3* fragments**

A *BamH I*/*Sal I* (the *Sal I* site is located on the vector) fragment was excised from pGEM-*MYR1-3* (sense orientation) and cloned into pGBKT7, the DNA-BD vector in BD Matchmarker Two-Hybrid System (Clontech, Palo Aito, CA) using the same sets of restriction enzymes. To make an in-frame fusion of MYR1-3 with the GAL4 DNA-Binding Domain, the resulting plasmid DNA was digested by *BamH I*, partially filled in, and re-ligated. To generate pGBKT7- *MYR1-3* fragments, pGBKT7-*MYR1-3* was digested by *Pst I* (one *Pst I* site is located on the vector pGBKT7, the other *Pst I* site in the middle of *MYR1-3*), re-ligated to generate pGBKT7-*MYR1-3-N-terminus* (encoding the first 226 amino acids) or digested by *Nco I* (one *Nco I* site is located on the vector, the other in the middle of *MYR1-3*), re-ligated to generate pGBKT7-*MYR1-3-C-terminus* (encoding the last 282 amino acids). pGBKT7-*MYR1-3-C-terminus* was digested by *Pst I*, re-ligated to generate pGBKT7-*MYR1-3-middle* (encoding middle 107 amino acids, i.e., amino acids 119-226).

**Identification of *MYR1* and *MYR2* knockout mutants**

*MYR1* and *MYR2* T-DNA insertion lines were generated at the SALK Institute Genomic Analysis Laboratory (http://signal.salk.edu/cgi-bin/tdnaexpress). Insertions of the T-DNA in SALK_097342, SALK_022192, SALK_069046, and SALK_087886 were confirmed by sequencing the PCR products amplified from genomic DNA using a pROK2 T-DNA left border primer 5'-GCGTGGACCGCTTGCTGCAACT-3 and a *MYR1* sense primer (for SALK_097342) 5'-GTTCCTCAGAGGAAATGGCA-3' or an antisense *EcoR V* linker primer (for SALK_022192) 5'-GATATCTCAATTCCAGCTGAAACCATTT-3', or a *MYR2* sense primer (for SALK_069046 and SALK_087886) 5'-GCAAAGTTGCACCAAACCAA-3'. Homozygous *MYR1* or *MYR2* T-DNA lines were

identified by PCR analysis using primers amplifying *MYR1* or *MYR2* coding region (no PCR products were got), and a pROK2 T-DNA left border primer and a *MYR1* sense primer (for SALK_097342) or an antisense primer (for SALK_022192) or a *MYR2* sense primer (for SALK_069046 and SALK_087886) (these primer combinations gave PCR products). Double mutant *myr1myr2* was generated by crossing a homozygous *MYR1* T-DNA line with a homozygous *MYR2* T-DNA line. Homozygous double mutants were identified from the F2 generation by PCR analysis using primers amplifying *MYR1* and *MYR2* coding regions.

**RNA isolation and semi-quantitative RT-PCR**

RNA isolation and RT-PCR were carried out using the RNeasy Plant Mini Kit (Qiagen, Valencia, CA) and the RETROscript Kit (Ambion, Austin, Taxas) according to the manufacturers' instructions, respectively. PCR amplification was performed in 25-ul reaction with the following primers: for the analysis of overexpression of *MYR1* driven by CaMV 35S promoter, an upstream primer 5'-GTTCCTCAGAGGAAATGGCA-3', and a downstream primer 5'-GCAAATGTCGCTGTACCTCA-3' (for *MYR1-1*), or 5'-GAGCCTCTATCCTGAGCTCA-3' (for *MYR1-2*), or 5'-TGAGCTGCAAATGTCGCTCA-3' (for *MYR1-3*), which span the alternative splicing site of intron 6 in *MYR1*; for analysis of *MYR1* expression in *myr1* mutants, an upstream primer 5'-GTTCCTCAGAGGAAATGGCA-3' and a downstream *EcoR V* linker primer 5'-GATATCTCAATTCCAGCTGAAACCATTT-3'; for analysis of *MYR2* expression in *myr2* mutants, an upstream *BamH I* linker primer 5'-GGATCCATGTATTACCAAAACCAGCAC-3' and a downstream *Sma I* linker primer 5'-CCCGGGAAACTCTCTTTTAACTTTTTGG-3'; for analysis of *actin* (*ACT2/7*) expression (as a control), an upstream primer 5'-GGCCGATGGTGAGGATATTC-3 and a downstream primer 5'-CTGACTCATCGTACTCACTC-3'.

## Results

### *MYR1* and *MYR2* are phloem-specific G2-like family genes

To identify genes required for vascular tissue-specific functions, we performed a genome-wide comparative analysis of xylem, phloem-cambium, and nonvascular tissue-specific transcripts using the 24K GeneChip and found 18 predicted transcription factors with expression biased toward phloem-cambium. Among these predicated phloem-cambium-biased transcription factors, 5 G2-like family members, At1g79430 (APL) (Bonke et al., 2003), At2g03500, At3g04030, At3g12730, and At5g18240 (MYR1) (Thelander et al., 2002), were noted (Zhao et al., 2005). According to Riechmann et al. (2000), the G2-like family belongs to the GARP superfamily, which was named after maize GOLDEN2 (Hall, et al., 1998), the ARR B-class proteins (Sakai et al., 1998) from Arabidopsis, and Chlamydomonas Psr1 (Wykoff et al., 1999). Members of the G2-like family possess one copy of the MYB DNA-binding domain. The G2-like family consists of about 42 members including KANADI1-4 (Kerstetter et al., 2001; Emery et al., 2003) and GLK1-2 (Fitter et al., 2002), in addition to APL and MYR1 mentioned above. The exact size of the G2-like family is not yet clear. For example, J. Sheen at Harvard Medical School listed 42 G2-like genes (http://genetics.mgh.harvard.edu/sheenweb/AraTRs.html), DATF at Peking University, China included 43 members (http://datf.cbi.pku.edu.cn/browsefamily.php?familyname=GARP-G2-like), and AtTFDB at the Ohio State University identified 44 members (http://arabidopsis.med.ohio-state.edu/AtTFDB/AtTFBrowseResults.jsp?fam=G2-like). KANADI1-4, APL, and GLK1-2 are required for establishment of polarity in the lateral organ (Kerstetter et al., 2001; Emery et al., 2003), phloem identity (Bonke et al., 2003), and chloroplast development (Fitter et al., 2002), respectively. These results suggest that G2-like family members play important roles in a variety of plant development processes. *MYR1* was isolated previously by screening for clones that can activate glucose repression in the absence of glucose in yeast (Thelander et al., 2002). MYR1 has not been characterized *in planta*. Among the 5 phloem-cambium-biased G2-like gene family members, *MYR1* displayed the highest expression level (Zhao et al., 2005). Sequence alignment and phylogenetic analysis of the G2-like family showed that At3g12730 and At3g04030 share the highest homology of the amino acid sequence with APL and MYR1, respectively (Fig.

3.1). A WU-BLAST 2.0 search (www.arabidopsis.org) showed that At3g04030 shares 78% identity in the amino acid sequence with MYR1, higher than all other G2-like family members. We refer to At3g04030 as MYR2.

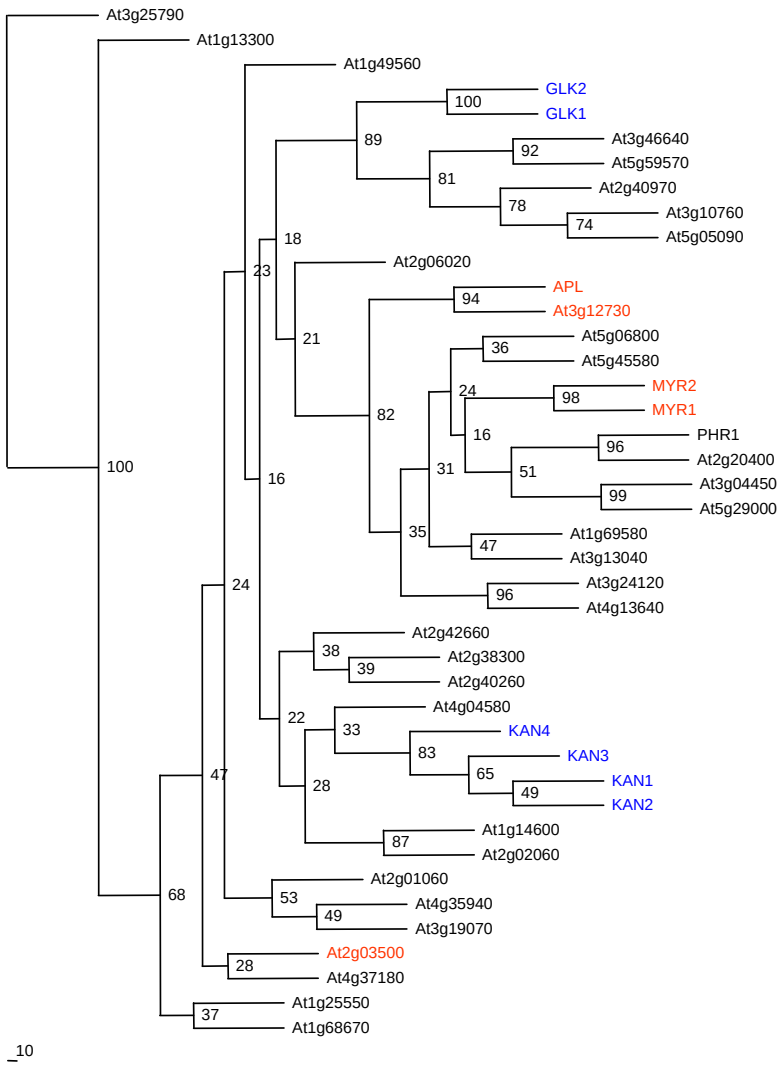


**Figure 3.1**. Phylogenetic analysis of the G2-like family in Arabidopsis. Phloem-cambium-biased genes (Zhao et al., 2005) are highlighted in red, and KANADI and GLK genes in blue. AGI identification number and corresponding accession number for amino acid sequences used are as follows: At1g13300, NP_563926; At1g14600, NP_172912; At1g25550, NP_564236; At1g32240 (KAN2), NP_564392; At1g49560, NP_564549; At1g68670, NP_564938; At1g69580, NP_177117; At1g79430 (APL), NP_849905;

At2g01060, NP_973385; At2g02060, NP_565281; At2g03500, NP_027544; At2g06020, NP_178659; At2g20400, NP_179630; At2g20570 (GLK1), NP_565476; At2g38300, NP_181364; At2g40260, NP_181555; At2g40970, NP_181630; At2g42660, NP_181794; At3g04030 (MYR2), NP_974216; At3g04450, NP_187095; At3g10760, NP_187687; At3g12730, NP_187879; At3g13040, NP_974298; At3g19070, NP_188537; At3g24120, NP_974356; At3g25790, NP_566778; At3g46640, NP_190248; At4g04580, NP_192367; At4g13640, NP_567408; At4g17695 (KAN3), NP_567535; At4g28610 (PHR1), NP_194590; At4g35940, NP_195319; At4g37180, NP_849513; At5g05090, NP_196128; At5g06800, NP_196298; At5g16560 (KAN1), NP_568334; At5g18240 (MYR1), NP_974799; At5g29000, NP_568512; At5g42630 (KAN4), NP_199077; At5g44190 (GLK2), NP_199232; At5g45580, NP_199371; At5g59570, NP_200765. The phylogram was generated using CLUSTALW 1.8 (http://clustalw.genome.jp), PHYLIP-3.63 (http://evolution.genetics.washington.edu/phylip.html), and TreeView 1.6.6 (http://taxonomy.zoology.gla.ac.uk/rod/treeview.html).

The 24K GeneChip data indicated that both *MYR1* and *MYR2* are phloem-specific, i.e., signals for these genes were scored as absent from xylem and nonvascular tissues (Zhao et al., 2005). To evaluate expression of *MYR1* and *MYR2* using an independent method, 1.471- and 2.008-kb regions upstream of the MYR1 and MYR2 translation start, the putative promoters of *MYR1* and *MYR2*, *MYR1p* and *MYR2p*, were fused to beta-glucuronidase (GUS) and/or smGFP (Chisholm et al., 2001) reporter genes, respectively. More than fifty (for GUS) or ten (for GFP) independent transgenic plants were analyzed. The results showed that GUS activity and GFP were observed throughout the vascular system where it was localized to phloem cells. In seedlings, GUS activity was not observed in the root tip, elongation or maturation zone, but was visible in older root tissue concomitant with the earliest stage of secondary phloem development. This expression pattern suggests that *MYR1* does not express in protophloem of roots. Higher levels of GUS staining were observed in leaves than in roots (Fig. 3.2).

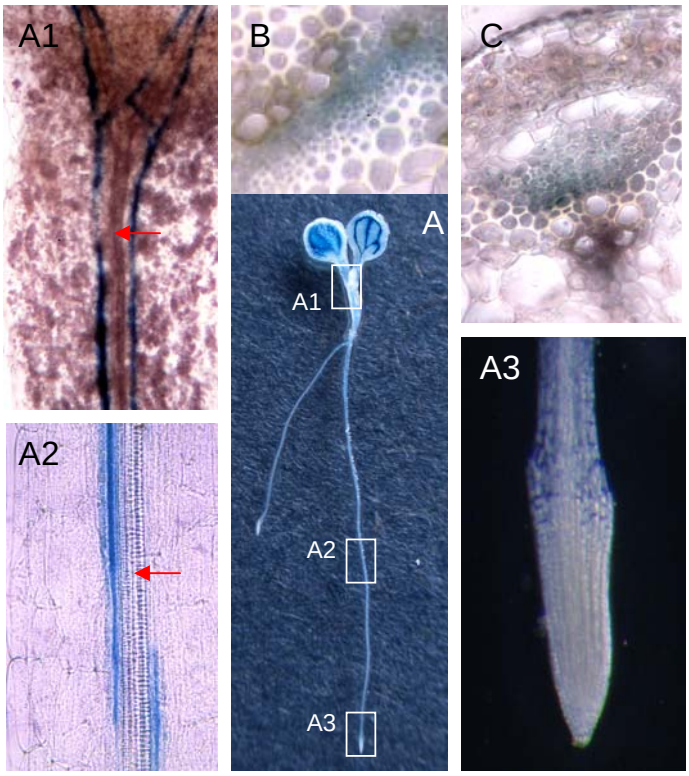


**Figure 3.2**. The *MYR1* promoter directs GUS expression in phloem cells. More than 50 independent T1 plants were analyzed with similar results**.** A**,** GUS expression driven by the *MYR1* promoter was observed throughout the vascular system in a six-day-old seedling. A1-A3, Enlarged images of insets shown in A, GUS activity was detected in phloem of older tissues (A1 and A2) but not the root tip (A3). Note peripheral (phloem) localization of GUS staining versus centrally localized xylem (arrows). B and C, GUS activity was localized to the abaxial (phloem) side of the vascular bundle in a transverse section of a petiole from an eight-week-old plant (B) and an inflorescence stem from a four-week-old plant (C).

**The structure of *MYR1* and *MYR2* genes**

We have isolated four isoforms of *MYR1* (*MYR1-1*, *MYR1-2*, *MYR1-3*, and *MYR1-4*) by a PCR-based screening strategy (see "Materials and Methods"). Among these four isoforms, three are resulted from alternative 3' splicing of intron 6 and have been previously reported (www.arabidopsis.org), *MYR1-1* (At5g18240.1 or At5g18240.4); *MYR1-2* (Thelander et al.,

2002; At5g18240.2 or At5g18240.3); *MYR1-3* (At5g18240.5). The alternative 3' splicing of intron 6 results in a deletion of 6 and 2 amino acids in MYR1-2 and MYR1-3, respectively, compared with MYR1-1 (Fig. 3.3 and 3.5). Compared with *MYR1-1*, the new isoform (*MYR1-4*) includes introns 2-5 and part of intron 6 (21-24 bp) and deletes part of exon 7 (42-45 bp), resulting in a frameshift predicted to produce a truncated protein (Fig. 3.4 and 3.5).

Even though retention of an unspliced intron in a fraction of transcripts is common in plants (Lorkovic et al., 2000), the intron unique to *MYR1-4* was spliced out using unusual splicing sites, i.e., the splicing sites in this isoform were not conserved and could not be predicted by software, such as SplicePredictor (http://bioinformatics.iastate.edu/cgi-bin/sp.cgi) and NetPlantGene (http://www.cbs.dtu.dk/services/NetPGene/). It is possible that this isoform was produced by defects of the spliceosome in old phloem tissue.

Like other MYB-related proteins, MYR1 contains a MYB repeat located between amino acids 47 and 98 predicted by Pfam (http://pfam.wustl.edu/hmmsearch.shtml). COILS (http://www.ch.embnet.org/software/COILS_form.html) detected a coiled-coil sequence in the middle of MYR1 (located between amino acids 149 and 169 for MYR1-1, 149 and 172 for MYR1-2, and 149 and 171 for MYR1-3, respectively). A coiled-coil sequence is a potential dimerization motif. The alternative 3' splice sites of intron 6 in *MYR1-1*, *MYR1-2*, and *MYR1-3* were located in the coiled-coil sequence. The alternative splicing did not disrupt the coiled-coil motif based on the prediction by COILS even though it resulted in a deletion of 6 and 2 amino acids in MYR1-2 and MYR1-3, respectively, compared with MYR1-1 (Fig. 3.3). The Arabidopsis genome includes 15 proteins containing both a MYB repeat and a coiled-coil region. These proteins comprise the MYB-CC family proposed by Rubio et al. (2001).

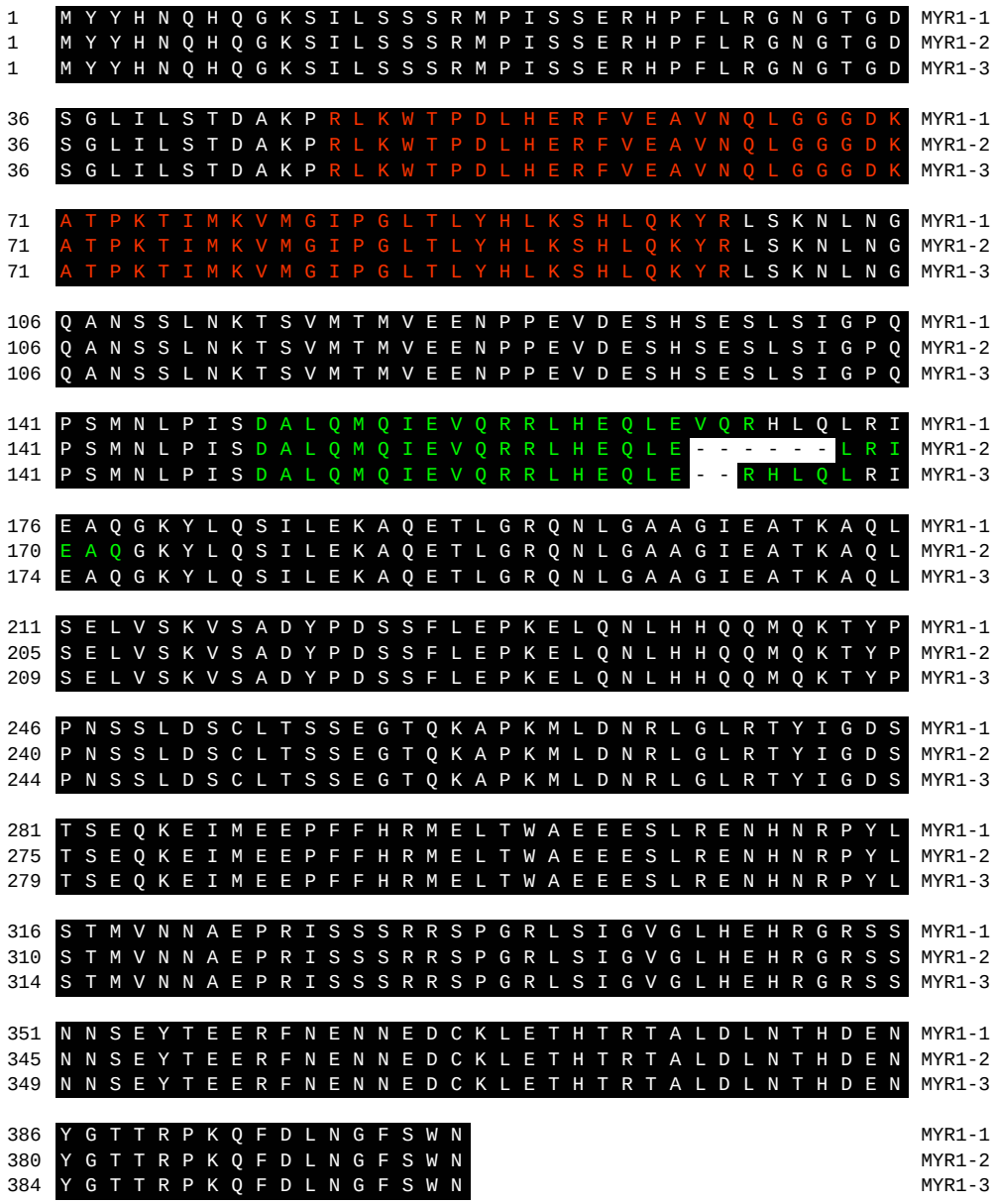


**Figure 3.3**. Multiple sequence alignment of MYR1 isoforms generated from alternative 3' splicing of intron 6. Residues that are identical to MYR1-1 are shaded with solid black. The MYB repeats are highlighted in red and the putative coiled-coil sequences in green. Gaps marked by dashes are caused by the alternative 3' splicing of intron 6. The multiple sequence alignment was produced with Lasergene (DNASTAR, Madison, WI).

```
M  Y  Y  H  N  Q  H  Q  G  K  S  I  L  S  S  S  R  M  P  I  S  S  E  R  H  P  F  L  R  G
ATGTATTACCACAACCAGCACCAAGGAAAGAGCATCCTCTCTTCATCGAGAATGCCCATTTCTTCTGAAAGGCATCCGTTCCTCAGAGGA

 N  G  T  G  D  S  G  L  I  L  S  T  D  A  K  P  R  L  K  W  T  P  D  L  H  E  R  F  V  E
AATGGCACAGGAGATTCTGGACTCATTCTCTCCACTGATGCAAAGCCACGACTAAAATGGACTCCAGATCTTCACGAGAGATTTGTTGAA

 A  V  N  Q  L  G  G  G  D  S  K  L  S  Y  K  Q  M  N  H  L  L  Q  S  G  F  L  N  I  M  Y
GCGGTCAACCAGCTTGGAGGAGGAGATAGTAAGTTATCTTATAAGCAAATGAACCATCTTTTACAATCAGGCTTTTTGAACATAATGTAT
                           II
 *
TAATGTGTATACTTTTGTCTGCGCAGAGGCTACTCCTAAGACAATCATGAAAGTCATGGGCATTCCAGGCCTTACCTTATACCATCTCAA

GAGTCATCTTCAGGTAATCCATCAACACTTTATACAGTCATATGCCCAAGGCCCTAAACTTACATGACTCGTTCATCAATTCGATTGGTA
          III
GAAAACTATTAAAGTAGCACAAAAATGACGATATGTCAAGATATGAAAAATCTGTAATATCTGTTTTTTGTTTTACAAAGATTATTAATA

TCATGATTTGACTACCAGAAATATAGGCTAAGCAAGAATCTTAATGGACAAGCTAACAGCAGTTTAAACAAGACAAGTAAGCTTAGTTAT
                                                                                IV
TCATTACTCAGATACAAAAATATTTTAATCTAAAGATTCATTCTTTTTTCATACTATTTTCCTTCAAGTAAACTAAAAGCAACCTGGTTT

AGGTGTGATGACCATGGTAGAAGAAAACCCCCCTGAAGTAGACGAAAGTCACAGTGAGAGTTTAAGCATTGGACCACAGCCGAGCATGTA
                                                                                          V
AGGATATGCCTATTTGCTTACATATTCTACCTTAGTAGATTCTCAAAAATGACCTATATTTGTGCACGCAGGAACTTACCCATAAGTGAT

GCCCTTCAAATGCAAATAGAGGTCCAGAGACGGCTACACGAGCAACTTGAGGTATCTATCATATACTGTACTCTG..............
                                                  VI
..............................................................................................

..............................................................................................

................................CAATCGATTCTGGAGAAAGCACAAGAGACTCTTGGAAGACAGAACCTAGGTGCAGC

TGGGATTGAAGCAACAAAAGCTCAACTCTCAGAATTAGTATCTAAAGTATCAGCAGACTATCCAGACTCTAGTTTCCTCGAACCGAAAGA

ACTGCAGAATCTACACCATCAACAGATGCAAAAAACGTATCCACCTAACTCCTCCCTGGACAGTTGCCTAACCTCAAGTGAAGGAACTCA

GAAAGCCCCAAAGATGCTTGACAACAGACTGGGATTAAGAACATATATTGGAGATTCAACTTCAGAGCAGAAAGAGATAATGGAAGAGCC

ATTCTTCCATAGAATGGAGCTCACATGGGCAGAAGAAGAAAGCCTCAGAGAGAATCACAACAGGCCATATCTTTCAACAATGGTTAACAA

CGCAGAACCGAGAATCTCGTCTTCAAGAAGAAGTCCTGGAAGATTGTCAATAGGAGTGGGATTACATGAACACAGAGGAAGGAGTAGCAA

CAACAGTGAGTATACAGAAGAAAGATTCAACGAGAATAATGAAGATTGCAAGCTTGAAACACACACAAGAACAGCTCTAGATCTTAACAC

ACACGACGAAAACTATGGCACAACGCGTCCTAAACAGTTTGATTTAAATGGTTTCAGCTGGAATTGA
```

**Figure 3.4**. *MYR1-4* DNA and the deduced protein sequence. Dots indicate the nucleotides spliced out as an intron in *MYR1-4* compared with the genomic DNA (www.arabidopsis.org). Nucleotides or dots underlined and marked as II to VI indicate introns II to VI of *MYR1-1*. The deduced protein sequence of *MYR1-4* was generated using JavaScript DNA Translator 1.1 (http://www.bioinformatics.vg/bioinformatics_tools/JVT.shtml).

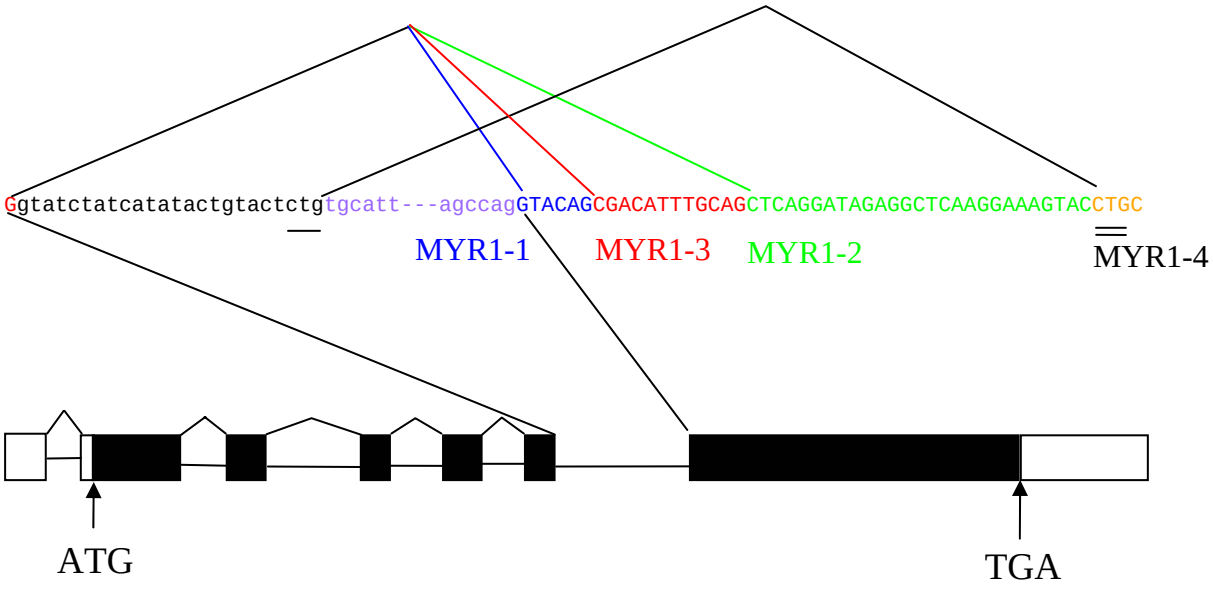


**Figure 3.5.** Scheme of alternative splicing of *MYR1* transcripts. The exons of *MYR1-1* are represented by boxes (protein-coding exons by black boxes and untranslated regions by white boxes) or capital letters; the introns of *MYR1-1* by lines or small letters. The 3' splice sites of intron 6 for *MYR1-1*, *MYR1-2*, and *MYR1-3* are located between purple- and blue-colored nucleotides, between red- and bright green-colored nucleotides, and between blue- and red-colored nucleotides, respectively. The fourth transcript, *MYR1-4*, retains introns 2-5. The 5' splice site of the unique intron in *MYR1-4* is located approximately at the ctg marked by a single underline, and its 3' splice site is located approximately at the CTG marked by double underlines. Because these nucleotides, ctg, are repeated at the splice sites and these splice sites can not be predicted by software, such as SplicePredictor (http://bioinformatics.iastate.edu/cgi-bin/sp.cgi) and NetPlantGene (http://www.cbs.dtu.dk/services/NetPGene/), the exact splicing sites are not yet known. Dashes indicated the nucleotides omitted to simplify the scheme.

We have isolated three isoforms of *MYR2* (*MYR2-1.1*, *MYR2-2.1*, and *MYR2-3.1*) by a PCR-based screening strategy. These three isoforms of *MYR2* were generated from alternative 3' splicing of intron 4. Among these three isoforms, *MYR2-2.1* (At3g04030.1) has been reported (www.arabidopsis.org). The remaining two isoforms, *MYR2-1.1* and *MYR2-3.1*, are new. The fourth isoform (At3g04030.2, we refer to it as *MYR2-1.2*) has been reported (www.arabidopsis.org) (Fig. 3.6 and 3.7). Since alternative splice sites of introns 1 and 4 could produce two and three isoforms, respectively, it is possible that *MYR2* has six isoforms (Fig. 3.7).

Like MYR1, MYR2 contains a MYB repeat (located between amino acids 47 and 98 for MYR2-1.1, MYR2-2.1, and MYR2-3.1, and 47 and 97 for MYR2-1.2) predicted by Pfam and a coiled-coil sequence (located between amino acids 149 and 169 for MYR2-1.1, 148 and 168 for MYR2-1.2, 149 and 172 for MYR2-2.1, and 149 and 171 for MYR2-3.1, respectively) predicted by COILS. Compared with MYR2-1.1, alternative splicing of introns 1 and 4 resulted in a deletion of one amino acid and a substitution (from A to T) in the MYB repeat of MYR2-1.2 and a deletion of 6 and 2 amino acids in the coiled-coil sequences of MYR2-2.1 and MYR2-3.1, respectively (Fig. 3.6), but the alternative splicing did not disrupt these domains/motifs, at least based on the prediction by Pfam and COILS, respectively.

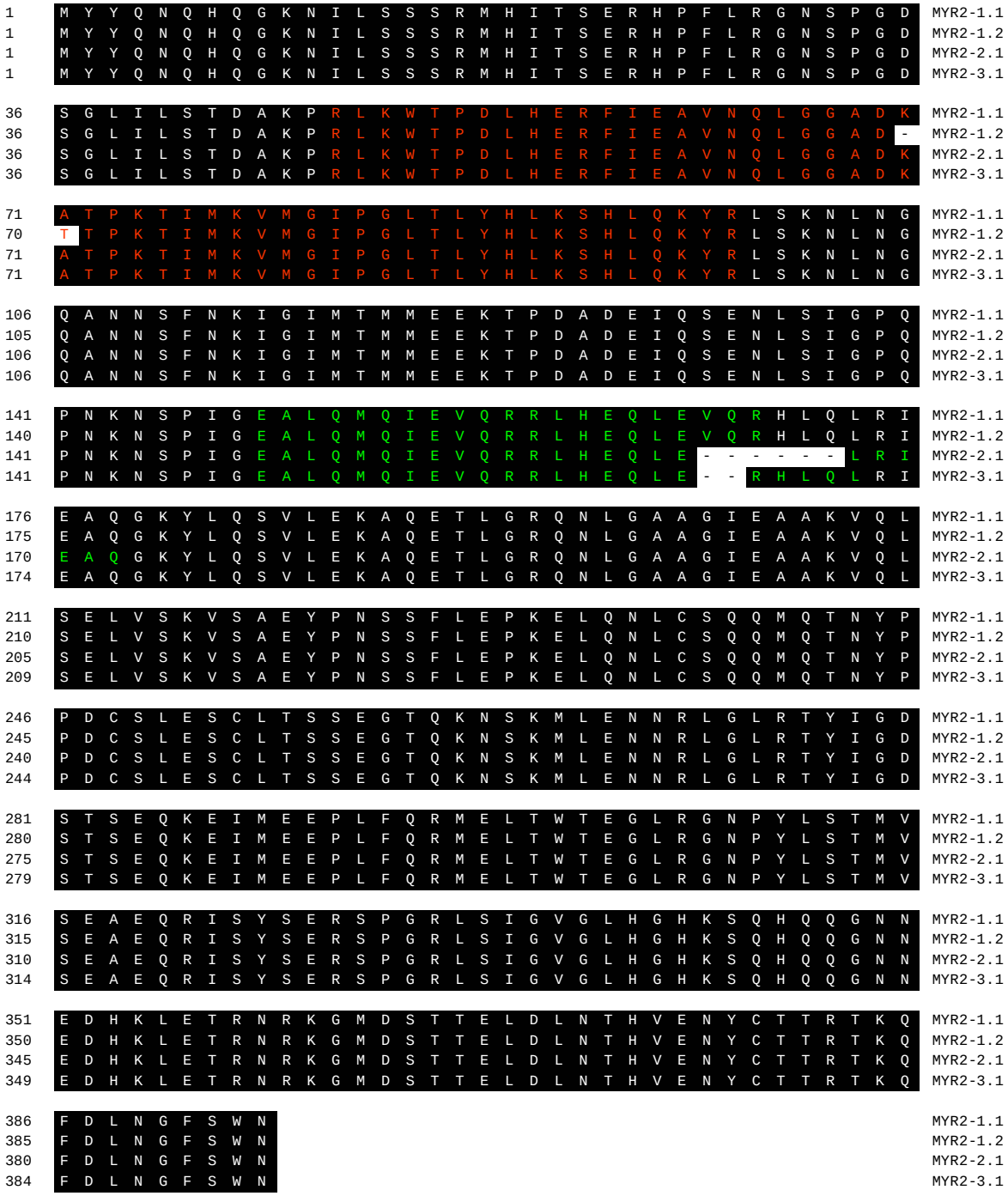


**Figure 3.6**. Multiple sequence alignment of MYR2 isoforms produced from alternative 3' splicing of introns 1 and 4. Residues that are identical to MYR2-1.1 are shaded with solid black. The MYB repeats are highlighted in red and the putative coiled-coil sequences in

green. Gaps marked by dashes indicate deletions resulted from the two alternative splicing sites. The multiple sequence alignment of MYR2 isoforms was produced using Lasergene

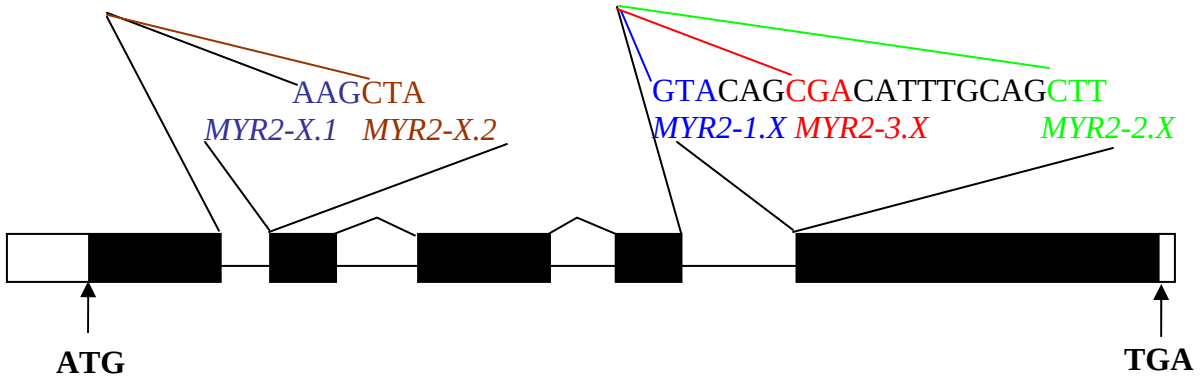


**Figure 3.7.** Scheme of the alternative splicing of the six *MYR2* transcripts. The exons and introns of *MYR2* are represented by boxes (protein-coding exons by black boxes and untranslated regions by white boxes) and lines, respectively. The isoforms generated from the alternative 3' splicing of intron 4 are termed as *MYR2-1.X*, *-2.X*, and *-3.X* for comparison with *MYR1-1*, *-2*, and *-3*, respectively where X can be either isoform generated from the alternative 3' splicing of intron 1. The isoforms produced from the alternative 3' splicing of intron 1 are named as *MYR2-X.1* and *MYR2-X.2* where X can be any of the three isoforms generated from the alternative 3' splicing of intron 4. The first three nucleotides of exon 5 for *MYR2-1.X*, *-2.X*, and *-3.X*, and of exon 2 for *MYR2-X.1* and *–X.2* are highlighted in blue, bright green, red, indigo, and brown, respectively.

**Nuclear localization of MYR1-3-GFP fusion protein**

Previous experiments by other investigators showed that several members of the G2-like family, such as G2 (Hall et al., 1998), PHR1 (Rubio et al., 2001), and APL (Bonke et al., 2003), localized to the nucleus. No NLSs were present in MYR1-1, -2, and -3 and MYR2-1.1, -1.2, -2.1, and -3.1 predicated by PredictNLS (http://cubic.bioc.columbia.edu/predictNLS/). To test whether MYR1 is localized in the nucleus, transgenic plants carrying a *MYR1-3-GFP* gene expression under the control of the *MYR1* promoter or the CaMV 35S promoter were generated. For comparison, *GFP* alone

driven by the *MYR1* promoter or the CaMV 35S promoter was used as a control. Microscopic analysis showed that MYR1-3-GFP fluorescence was observed in the nucleus (driven by *MYR1p* or 35S promoter), whereas in the transgenic plants carrying the control construct (*MYR1p-GFP* or *35S-GFP*), fluorescence was observed throughout the phloem sieve cells (driven by *MYR1p*) (data not shown) or the cytosol (driven by 35S promoter) (Fig. 3.8). This finding suggests that MYR1-3 contains a nuclear localization signal.

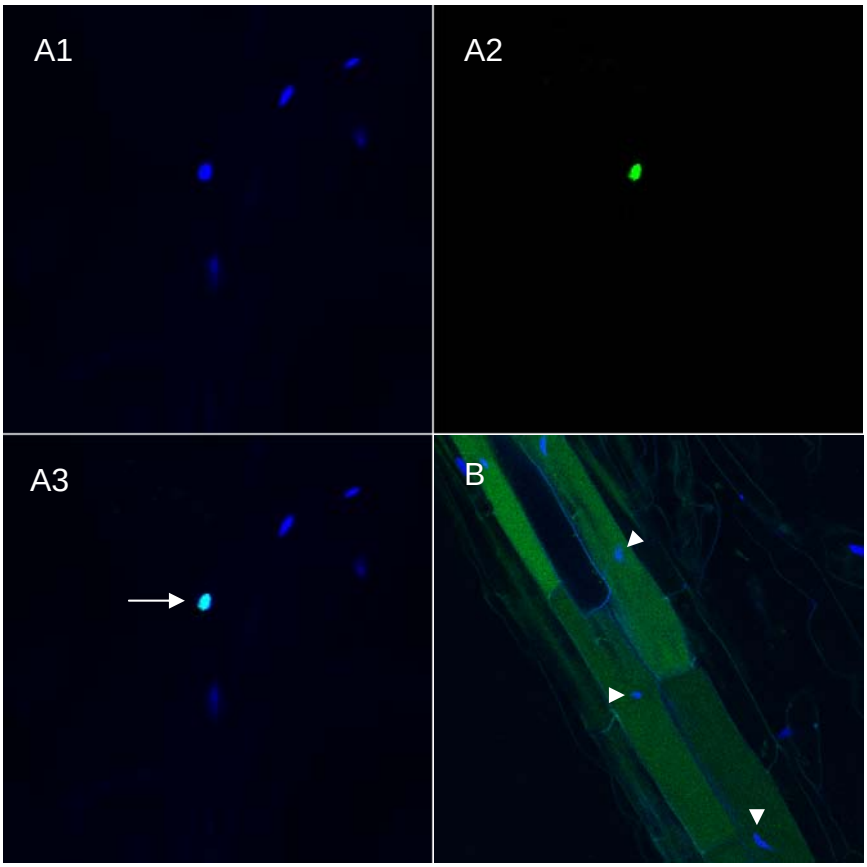


**Figure 3.8.** MYR1-3-GFP fluorescence is observed in the nucleus. *35S-MYR1-GFP* expression pattern in a root from a three-week-old transgenic Arabidopsis plant (arrow in A3). A3 panel shows the merge of A1 (the nucleus stained by Hoechst 33342) and A2 (MYR1-GFP fluorescence). GFP fluorescence in the control plants transgenic for *35S-GFP* is observed through the cells and does not localize to nuclei (arrowheads in B). Images were obtained using a Zeiss laser scanning confocal microscope (LSM 510).

**The N- and C-termini of MYR1 have transactivation activity**

Previous investigations suggested that G2-like family members, such as G2, ZmGLK1, and PHR1, may function as transcription factors by binding DNA and regulating gene expression at the transcription level and that their transcription activation domains were located in the N-terminal portion (Rossini et al., 2001; Rubio et al., 2001). To test whether MYR1 contains a transcription activation domain, we made a series of constructs by fusing MYR1-3 full-length and truncated versions to the GAL4 DNA-binding domain and tested their transactivation activity in a yeast strain AH109 carrying four reporters (*ADE2*, *HIS3*, *MEL1*, and *lacZ*) under the control of three distinct GAL4 upstream activating sequences (UASs) and TATA boxes (Clontech). The results indicated that full-length MYR1-3 (1-400 aa), the N- (1-226 aa) and C- (119-400 aa) terminal portions could activate transcription and promoted yeast growth in the absence of histidine (Fig. 3.9) or adenine (data not shown), suggesting that both N- and C- termini of MYR1 have transactivation activity. This result contrasts with G2 and ZmGLK1 (Rossini et al., 2001) where only the N-terminal portion could transactivate in yeast.

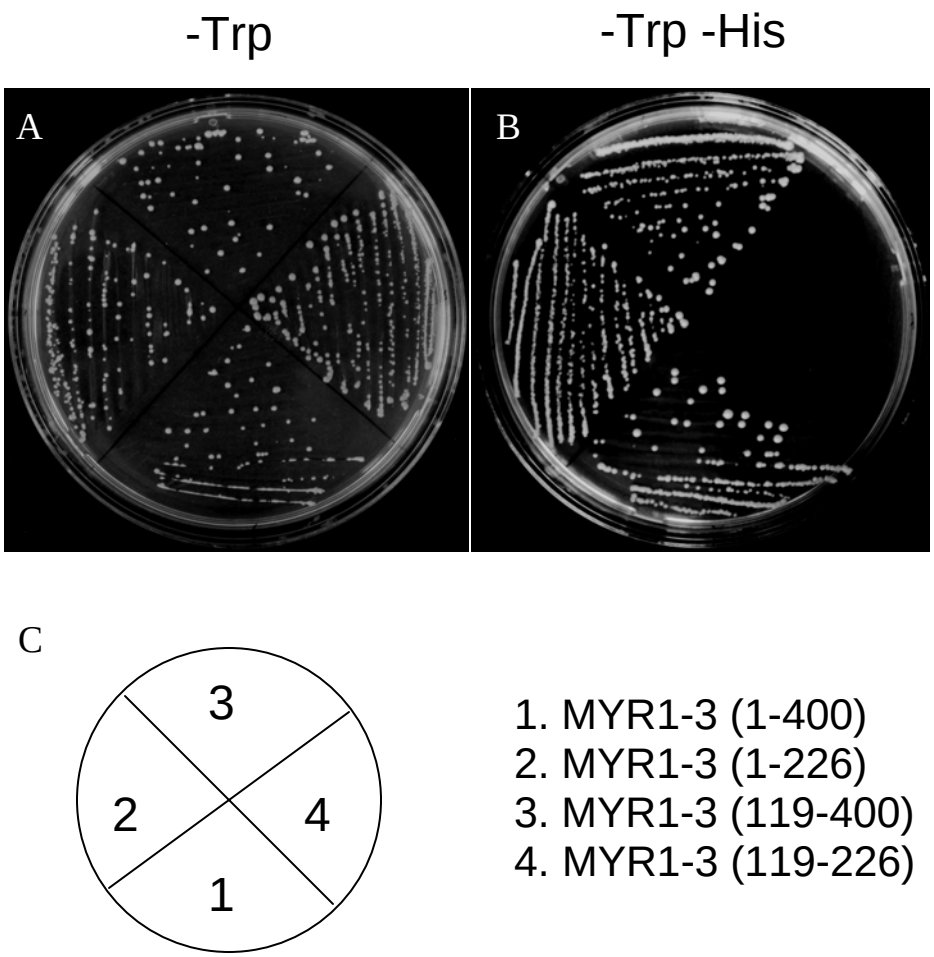


**Figure 3.9.** Identification of the transactivation domains of MYR1-3. MYR1-3 full-length (amino acids 1-400) and truncated versions encoding the first 226 amino acids, last 282 amino acids, and the middle 107 amino acids were fused in frame to the GAL4 DNA-binding domain in pGBKT7. Yeast cells (AH109) were transformed with the indicated plasmids, and streaked on plates lacking Trp (A, -Trp) or Trp and His (B, -Trp –His). C, Scheme showing positions of yeast transformed with plasmids containing MYR1-3 full-length and truncated versions as indicated.

**Loss-of-function of *MYR1*, *MYR2*, and *MYR1 MYR2***

**a) loss-of-function of *MYR1***

To obtain loss-of-function mutations in the *MYR1* gene, we identified two T-DNA insertion lines (SALK_097342 and SALK_022192). Sequence analysis revealed that the T-DNA insertion site in SALK_097342 (based on the T-DNA left border/plant genomic DNA junction) is located in the intron 4, 30 bp (not including microhomology) upstream from its 3' splice site. One bp of microhomology, C, was found at the transition point. The T-DNA insertion site in SALK_022192 is located in the last exon, 107 bp upstream from the translation termination codon. Two bp of microhomology, TT, were found at the transition point. We named these *myr1* insertion alleles *myr1-t1* and *myr1-t2*. RT-PCR indicated T-DNA insertion abolishes expression of the full-length *MYR1* mRNA in homozygous *myr1-t1* plants (Fig. 3.10). Plants homozygous for *myr-t1* or *myr1-t2* were not significantly different from wild type plants when grown under continuous light.

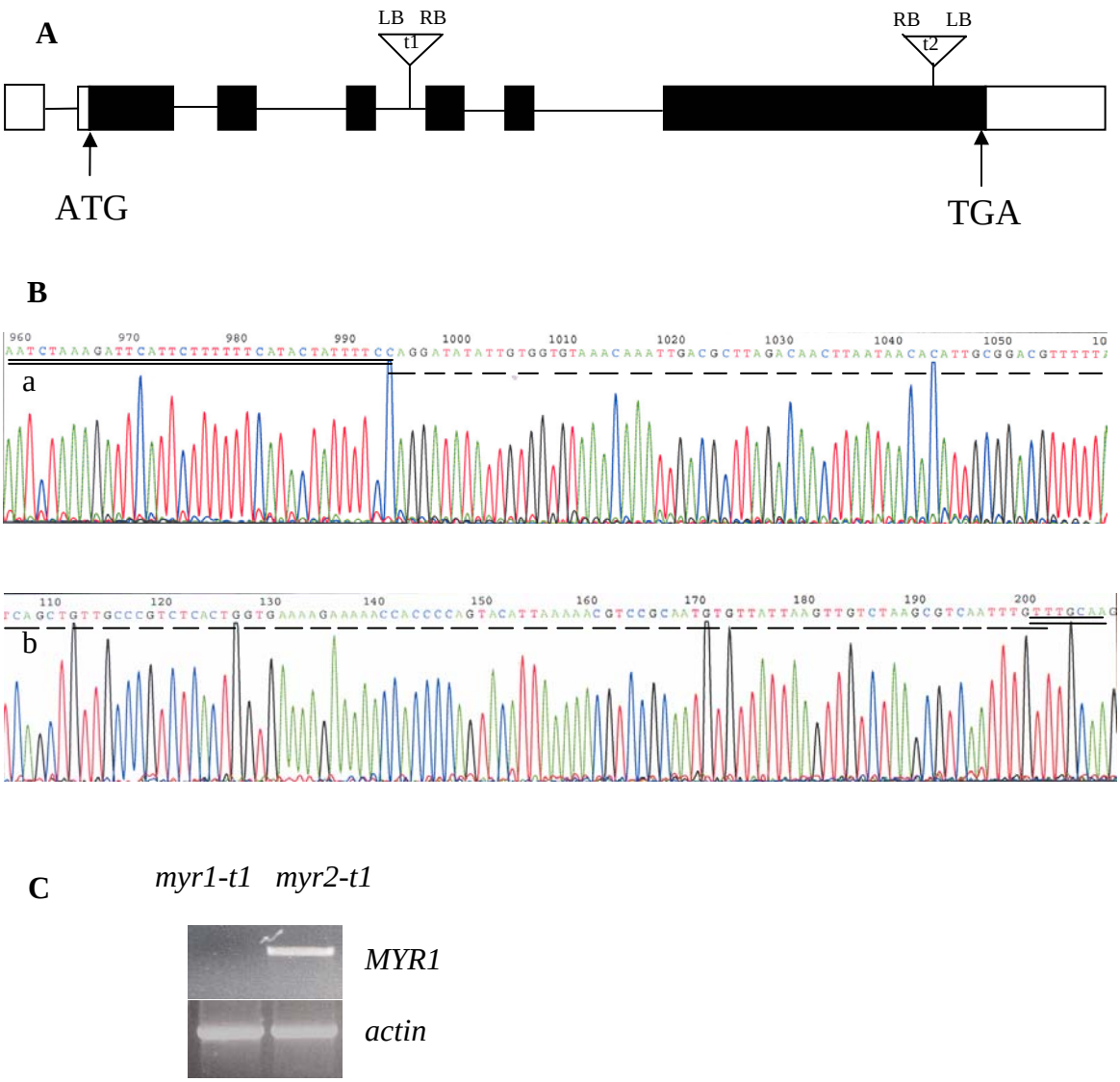


**Figure 3.10**. Characteristics of the *myr1* mutations. A, The positions of T-DNA insertion sites in the *myr1* insertion alleles *myr1-t1* and *myr1-t2*. Protein-coding exons of *MYR1* are represented by black boxes, untranslated regions by white boxes, and introns by lines. ATG, translation initiation codon; TGA, translation termination codon; LB, T-DNA left border; RB, T-DNA right border; t1, T-DNA insertion in *myr1-t1*; t2, T-DNA insertion in *myr1-t2*. B, Sequence analysis of junctions between T-DNA left border (dashes) and plant genomic DNA (double lines) in two *myr1* insertion alleles *myr1-t1*and *myr1-t2*. Microhomology (the C, position 994 in B.a and the TT, positions 202-203 in B.b indicated by overlapping dashes and double lines) was noted. C, Ethidium bromide-stained gels showing RT-PCR analysis of the expression of *MYR1* and *actin* in *myr1-t1* and *myr2-t1* plants (as a control).

**b) Loss-of-function of *MYR2***

Given that *myr1* mutants lack an obvious phenotype, i.e., they are indistinguishable from wild type plants, we asked whether there is a redundant gene in the Arabidopsis genome. Sequence alignment and phylogenetic analysis of the G2-like family showed that At3g04030 (MYR2) shares high homology with MYR1, and both MYR1 and MYR2 share lower levels of homology with other G2-like gene family members (Fig. 3.1).

To obtain loss-of-function mutations in the *MYR2* gene, we identified two T-DNA insertion lines (SALK_069046 and SALK_087886). Sequence analysis revealed that the T-DNA insertion site in SALK_069046 is located in intron 4, 47 bp upstream from its 3' splice site based on the sequence of *At3g04030.1* (www.arabidopsis.org). Three bp of microhomology, CAG, were found at the transition point. The T-DNA insertion in SALK_087886 is located in exon 2, 37 bp upstream from the 5' splice site of intron 2. Three bp of filler DNA, GAG, were found at the transition point. We named these two *myr2* insertion alleles *myr2-t1* (SALK_069046) and *myr2-t2* (SALK_087886). RT-PCR indicated that no full-length *MYR2* mRNA was detected in homozygous *myr2-t1* plants (Fig. 3.11). Under continuous light, the *myr2* knockout mutants flowered early with an average of 16.6 rosette leaves compared to 18.8 rosette leaves for wt plants but were otherwise not significantly different from wild type plants ( see the following discussion).

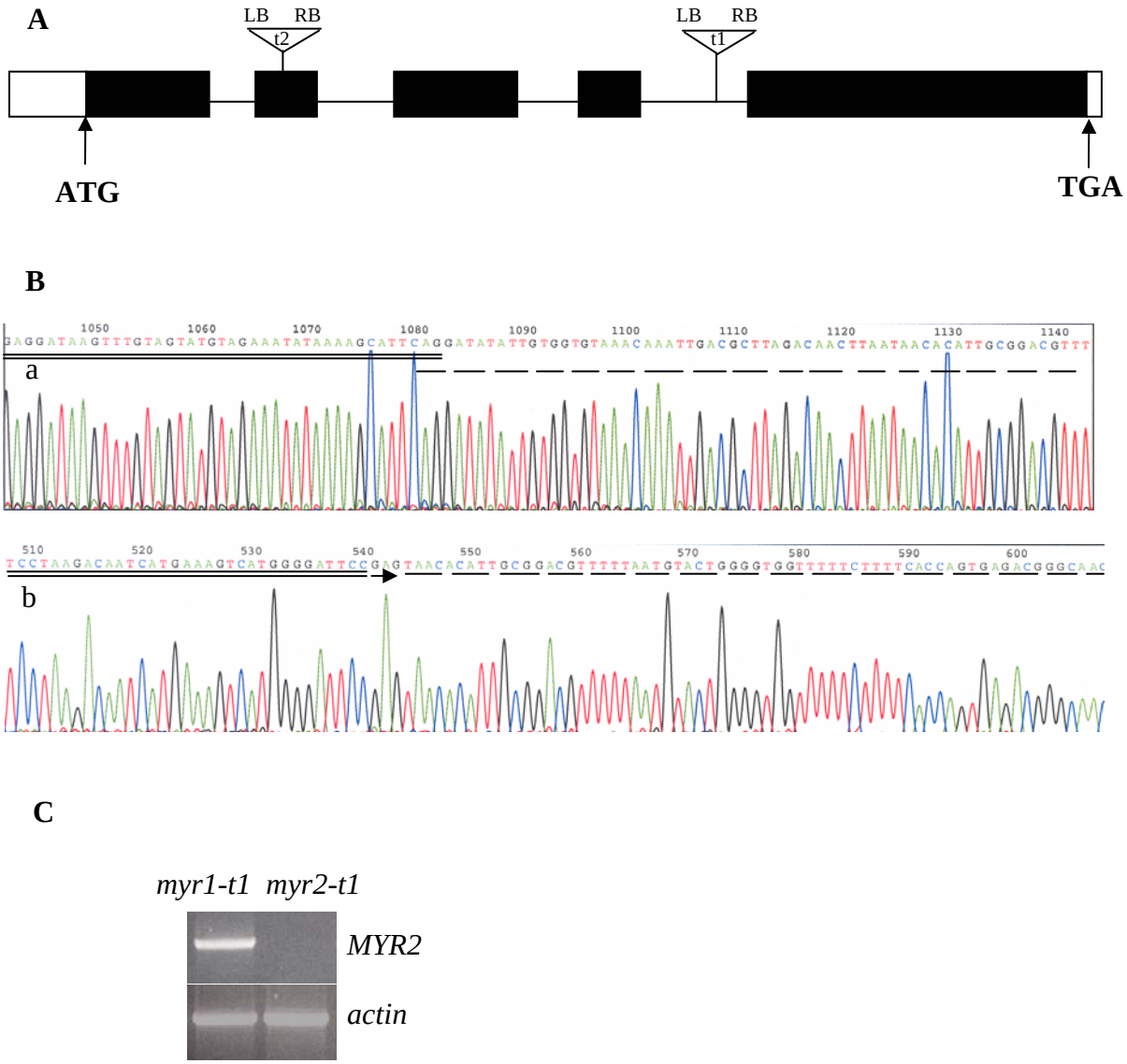


**Figure 3.11**. Characteristics of the *myr2* mutations. A, The positions of T-DNA insertion sites in the *myr2* insertion alleles *myr2-t1*and *myr2-t2*. Protein-coding exons of *MYR2* are represented by black boxes, untranslated regions by white boxes, and introns by lines. ATG, translation initiation codon; TGA, translation termination codon; LB, T-DNA left border; RB, T-DNA right border; t1, T-DNA insertion in *myr2-t1*; t2, T-DNA insertion in *myr2-t2*. B, Sequence analysis of junctions between T-DNA left border (dashes) and plant genomic DNA (double lines) in the *myr2* insertion alleles *myr2-t1* (B.a) and *myr2-t2* (B.b). Microhomology (the CAG, positions 1080-1082 indicated by overlapping dashes and double lines in B.a) or filler DNA (the GAG, positions 541-543 indicated by arrow in B.b)

was noted. C, Ethidium bromide-stained gels showing RT-PCR analysis of the expression of *MYR2* and *actin* in *myr1-t1* (as a control) and *myr2-t1* plants.

**c) Loss-of-function of *MYR1 MYR2***

Based on the following observations: 1) both *myr1* and *myr2* mutants lack an obvious phenotype (except *myr2* plants flower early, i.e. exhibited reduced number of rosette leaves at bolting), 2) MYR2 shares 78% identity at the amino acid level with MYR1, and 3) both *MYR1* and *MYR2* exhibit phloem-restricted expression, we asked whether *MYR1* and *MYR2* are redundant genes. We constructed two *myr1 myr2* double mutants, *myr1myr2_1* (described in this report) and *myr1myr2_2* (not yet analyzed), by crossing *myr1-t1* with *myr2-t1* and crossing *myr1-t2* with *myr2-t2*, respectively. The early flowering phenotype was slightly more pronounced in the *myr1myr2_1* plants in three independent experiments where 15.3 rosette leaves were present at the time of flowering versus 16.6, 18.4, and 18.9 rosette leaves for *myr2-t1*, *myr1-t1*, and wt plants, respectively. *myr1myr2_1* plants exhibited additional differences in development compared to wt and single mutant plants including elongated petioles, semi-erect leaf orientation and suppression of outgrowth of both secondary inflorescences and higher order branches on the primary inflorescence (i.e., increased apical dominance). Specifically, on eight-week-old plants, the average length of second-order branches on the primary inflorescence of *myr1myr2_1* plants was 14.9 cm compared to 23.7 cm for wt. Average second-order branch length for *myr1-t1* and *myr2-t1* plants was similar to that of wt plants at 23.6 cm and 26.0 cm, respectively. Third-order branch outgrowth was completely suppressed in *myr1myr2_1* plants, while wt, *myr1-t1* and *myr2-t1* plants produced an average of four third-order branches per plant ranging in length from 5.7 -7.9 cm. Outgrowth of one or two secondary inflorescences (average length = 14 cm) was observed for wt, *myr1-t1*, and *myr2-t1* plants, while only one in three *myr1myr2_1* plants produced elongated secondary inflorescences with an average length of only 1 cm (Fig. 3.12). Despite the fact that MYR1 and MYR2 are homologous to and share repression domains with APL, a known regulator of sieve element differentiation, *myr1myr2* mutants exhibited no obvious alteration in phloem development.

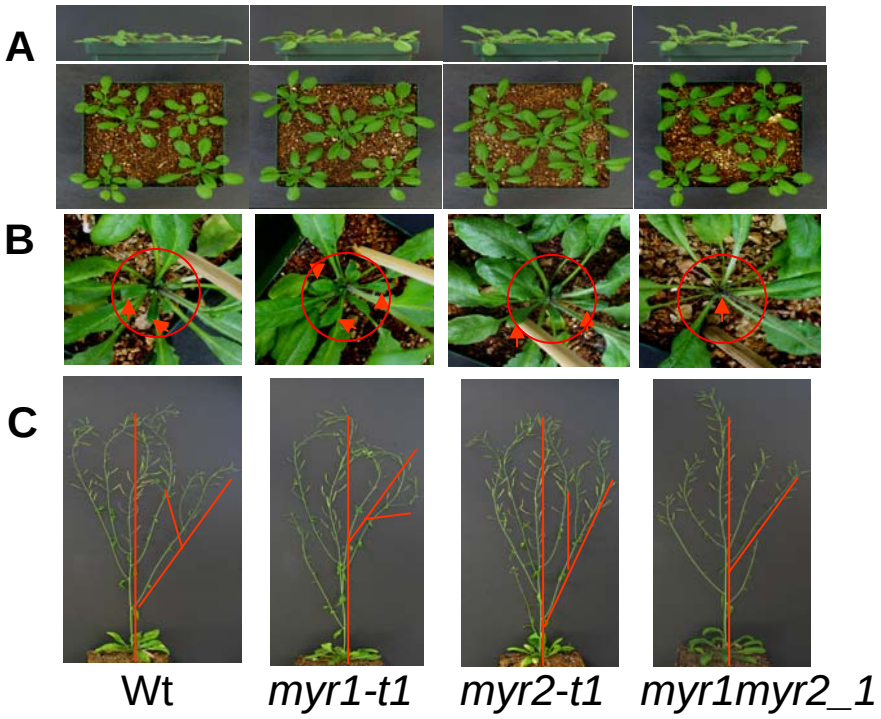
A
B
C
Wt
myr1-t1
myr2-t1
myr1myr2_1

**D**

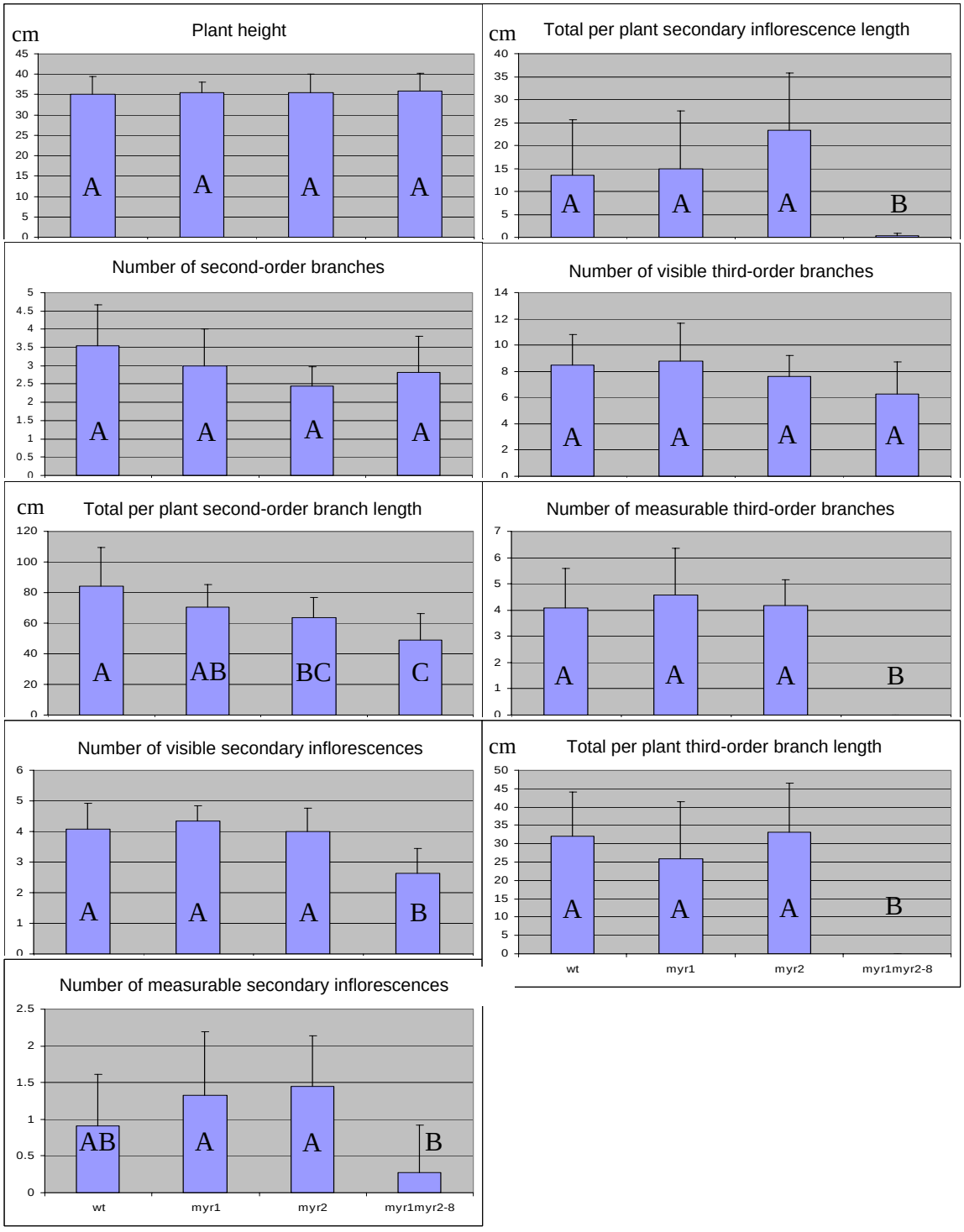
cm
Plant height
A
A
A
A
cm
Total per plant secondary inflorescence length
A
A
A
B
Number of second-order branches
A
A
A
A
Number of visible third-order branches
A
A
A
A
cm
Total per plant second-order branch length
A
AB
BC
C
Number of measurable third-order branches
A
A
A
B
Number of visible secondary inflorescences
A
A
A
B
cm
Total per plant third-order branch length
A
A
A
B
wt
myr1
myr2
myr1myr2-8
Number of measurable secondary inflorescences
AB
A
A
B
wt
myr1
myr2
myr1myr2-8

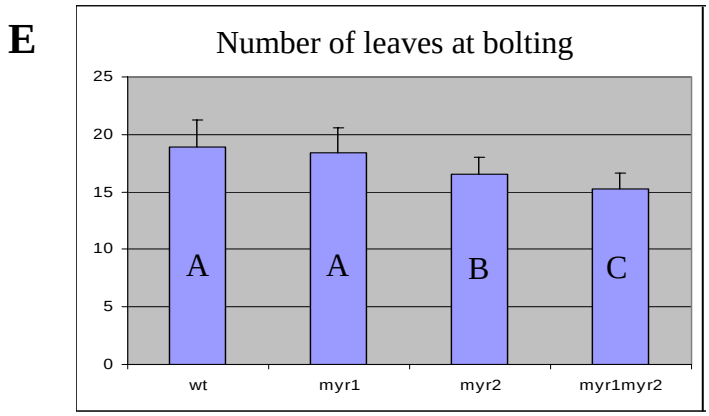


**Figure 3.12**. Phenotype of *MYR1*, *MYR2* single and double mutants

A, Wild type, *myr1-t1*, *myr2-t1*, and *myr1myr2_1* plants 4 weeks post-germination. Rosette leaves of *myr1myr2_1* plants exhibit a semi-erect growth habit compared to wild type and single mutant lines, *myr1-t1* and *myr2-t1*. B, Wild type, *myr1-t1*, *myr2-t1*, and *myr1myr2_1* plants 6 weeks post-germination. Outgrowth of secondary inflorescence buds, as indicated by advanced development of cauline leaves on secondary inflorescences, is blocked in *myr1myr2_1* mutants (arrows in red ovals). C and D, Wild type, *myr1-t1*, *myr2-t1*, and *myr1myr2_1* plants 8 weeks post-germination. Outgrowth of second-order branches is reduced while third-order branch growth is completely repressed in *myr1myr2_1* mutants (the primary inflorescence, and representative second and third-order branches are highlighted by red lines). E, Number of rosette leaves at bolting is reduced in *myr2* and *myr1myr2* plants. Error bars in D and E represent standard deviation (SD, n = 10 or 12 for each line in D, 24 for each line in E). Statistical analysis was performed according to ANOVA Model I as described (Neter et al., 1996). The means between Group A and Group B, or Group B and Group C are significantly different (with a 99 percent confidence level).

### *MYR1* and *MYR2* are functionally redundant in complementation experiments

To test whether *MYR1* and *MYR2* are functionally redundant, we introduced a 4.544 or 5.491-kb genomic DNA fragment, including 1.471-kb sequences upstream of the *MYR1* translation initiation codon, *MYR2* coding region (1.655-kb), and 1.418-kb sequences downstream of the *MYR1* termination codon or 2.008-kb sequences upstream of the *MYR2* translation initiation codon, *MYR1* coding region (1.957-kb), and 1.526-kb sequences downstream of the *MYR2* termination codon into *myr1myr2_1* double mutant background. For comparison, we also introduced a 4.846- or 5.189-kb genomic DNA of *MYR1* or *MYR2*, including 1.471-kb sequences upstream of the *MYR1* translation initiation codon, *MYR1* coding region (1.957-kb), and 1.418-kb sequences downstream of the *MYR1* termination codon or 2.008-kb sequences upstream of the *MYR2* translation initiation codon, *MYR2* coding region (1.655-kb), and 1.526-kb sequences downstream of the *MYR2* termination codon, and vector only into *myr1myr2_1* double mutant background. These results showed that introduction of the *MYR1* or *MYR2* genomic DNA driven by *MYR1* or *MYR2* promoter rescued the *myr1myr2* mutant in more than 93% transformants (specifically, 42 in 45 plants for *MYR1p-gMYR1-MYR1 3'*, 40 in 41 plants for *MYR1p-gMYR2-MYR1 3'*, 51 in 52 plants for *MYR2p-gMYR1-MYR2 3'*, 44 in 44 plants for *MYR2p-gMYR2-MYR2 3'*) except the earlier flowering phenotype. Preliminary results indicated that *myr1myr2* plants transformed with *MYR1p-gMYR2-MYR1 3'* or *MYR2p-gMYR2-MYR2 3'* biased to wt or *myr1* plants whereas *myr1myr2* plants transformed with *MYR1p-gMYR1-MYR1 3'*, *MYR2p-gMYR1-MYR2 3'* biased to *myr2* plants for the earlier phenotype, indicating that MYR1 and MYR2 are at least partially redundant.

### *myr1myr2* plants are more resistant to 5-methyl-tryptophan (5-mT)

*myr1myr2_1* phenotypes are reminiscent of shade-avoidance responses and *yucca*. Shade-avoidance responses in higher plants are controlled by the action of the phytochromes (Devlin et al., 2003). Recent investigations showed that auxin is implicated in the regulation of shade-avoidance responses (for review, see Morelli and Ruberti, 2002). *yucca* is a dominant Arabidopsis mutant with elevated levels of free auxin. Characterization of *yucca* revealed that *YUCCA* encodes a flavin monooxygenase-like enzyme, catalyzing the N-oxygenation of tryptamine, a rate-limiting step in tryptophan-dependent auxin

biosynthesis (Zhao et al., 2001). To indirectly test whether *myr1myr2_1* plants may have elevated capacity for tryptophan-dependent auxin production, we grew wt, *myr1-t1*, *myr2-t1*, and *myr1myr2_1* in media containing different concentration of 5-methyl-tryptophan (5-mT), a tryptophan analog whereby reported experiments used to characterize *YUCCA*. Preliminary results suggested that *myr1myr2_1* plants were more resistant to the toxic tryptophan analog and produced more adventitious roots compared with wt grown in media containing 50-μM 5-mT. Single mutant *myr1-t1* (Fig. 3.13) and *myr2-t1* (data not shown) plants produced adventitious roots similar to wt plants. These results suggest that MYR1 and MYR2 may be associated with tryptophan-dependent auxin biosynthesis through negative regulation.


**Figure 3.13.** *myr1myr2* plants are more resistant to 5-methyl-tryptophan (5-mT), a toxic tryptophan analog and produce more adventitious roots compared with wild type and single mutant *myr1-t1*. Seedlings were grown on 0.5XMS medium containing 50-μM 5-mT for one month.

### *MYR1* and *MYR2* overexpression results in downward curvature of true leaves and suppression of growth and lateral shoot formation and/or outgrowth

To further investigate the function of MYR1 and MYR2, we overexpressed *MYR1-1*, *-2*, and *-3* and *MYR2-1.1*, *-2.1*, and *-3.1* under the control of the CaMV 35S promoter. Two kinds of phenotypes were observed in all *MYR1* and *MYR2* overexpression experiments: one phenotype is similar to that observed in the *myr1myr2_1* double mutant, i.e., outgrowth of secondary inflorescences, basal second-order branches and all third-order branches were inhibited; the other (affecting 18.4%, 19.0%, and 6.8% of 50-100 transformants in *35S-MYR1-1*, *35S-MYR1-2*, and *35S-MYR1-3*, respectively) is more severe in that the second-order branch outgrowth and development were almost completely blocked. The severe phenotype plants were severely stunted and produced leaves that were curved toward the abaxial surface. The most severely affected plants were sterile and produced no seeds (Fig. 3.14). To investigate whether the severe phenotype was caused by the overexpression of the isoform, we performed semi-quantitative RT-PCR experiments for *35S-MYR1-3*. The results showed that the severe phenotype was correlated with the higher level of *MYR1-3* expression. Specifically, the severe phenotype plants had more than 100 fold higher expression level of *MYR1-3* compared with wild type-like plants, while, other naturally occurring isoforms, *MYR1-1* and *MYR1-2*, evaluated as controls, did not show any detectable difference between wild type-like and the severe phenotype plants. These results suggest a model where promotion of lateral shoot outgrowth mediated by MYR1 and MYR2 depends on formation of specific heterodimers consisting of isoforms of MYR1 and/or MYR2. In this model, overexpression or null mutants affecting dimer-dependent process could block function of not only MYR1 and MYR2, but also MYR1/MYR2 homologs, which depend on specific dimer combinations.

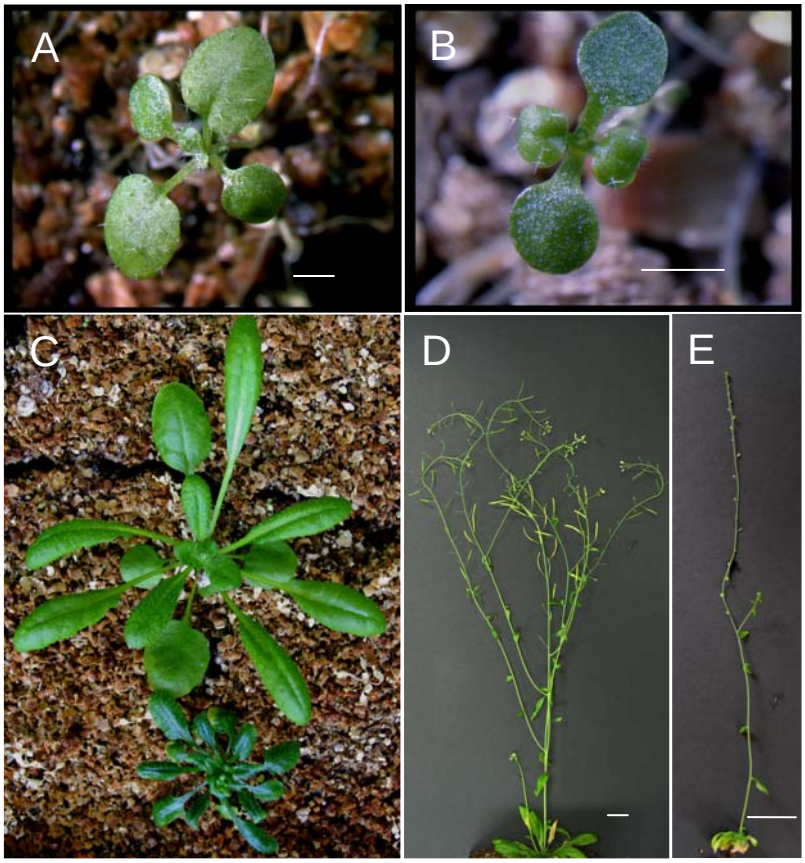


**Figure 3.14**. Overexpression of any one of the *MYR1* isoforms results in downward curvature of true leaves and suppression of growth and lateral shoot formation in the most severely affected individuals**.** Representative results from an *MYR1-1* overexpression experiment are shown here. A, 35S-*MYR1-1* wild type-like plant (2-week-old). B, *35S-MYR1-1* stunted plant (mutant). Note downward curvature of the true leaves. C, *35S-MYR1-1* mutant is shown near a wild type-like plant of the same age (4-week-old). D and E, *35S-MYR1-1* mutant (E) is compared with a wild type plant (D) of the same age (8-week-old). Bars= 1 cm (A, B, D, and E).

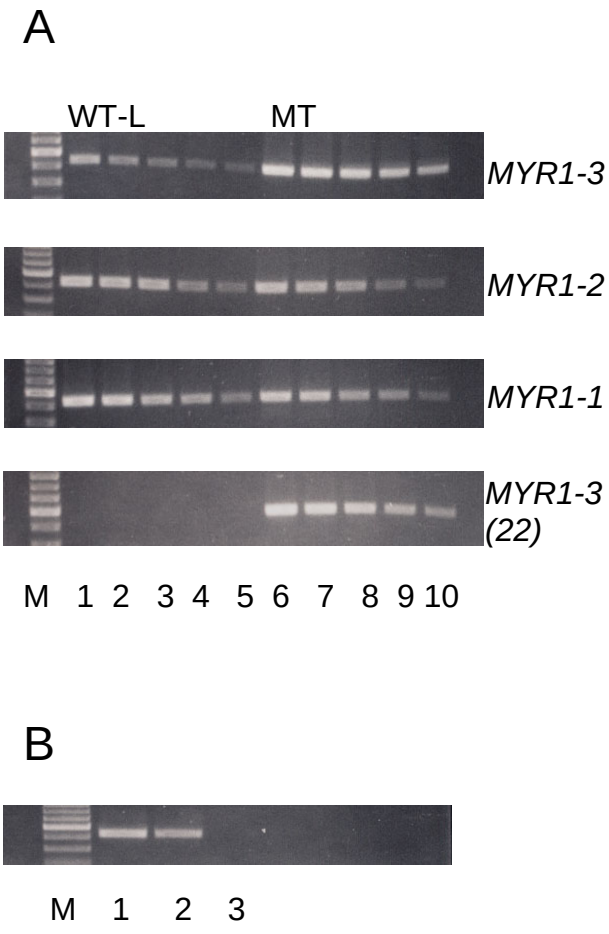


**Figure 3.15**. Ethidium bromide-stained gels showing products of semi-quantitative RT-PCR for *35S-MYR1-3* mutant (MT) and *35S-MYR1-3* wild type-like (WT-L) plants. A. cDNA from MT only for WT-L versus MT comparison of *MYR1-3* expression was diluted 16-, 32-, 64-, 128-, and 256-fold (lanes 6-10), the other cDNAs were diluted 1-, 2-, 4-, 8-, and 16-fold (lanes 1-5 or 6-10). B. Ethidium bromide-stained gels showing PCR products for *MYR1-1* (lane 1), *MYR1-2* (lane 2) expressed in WT-L plants, and water-only negative control (lane 3). Number of PCR cycles used for *MYR1-3* (22) is 22, whereas numbers of PCR cycles used for the other are 30. M in A and B indicates 100 bp DNA Ladder where brighter band = 500 bases.

## Discussion

### MYR1 and MYR2 are phloem-specific G2-like family members

Following dissection of root-hypocotyl segments into xylem, phloem-cambium, and nonvascular tissues, we performed genome-wide expression profiling of these tissues using the 24K GeneChip. From these transcript profiles, we identified 5 phloem-cambium-biased G2-like family members. Among them, *MYR1* displayed the highest expression level. MYR2 shared the highest homology with MYR1. To test their expression by an independent method, we fused their putative promoters with GUS and/or GFP reporter genes. As expected, GUS activity and GFP fluorescence were observed in phloem throughout the vascular system. By introducing *MYR1* or *MYR2* genomic DNA into *myr1myr2* double mutants, we showed in promoter-swapping experiments that *MYR1* or *MYR2* coding regions, driven by either promoter, both of which were shown to direct phloem-specific expression of the beta-glucuronidase (GUS) or GFP reporter gene, rescued the wild type phenotype in T1 transformants. These results indicate that *MYR1* and *MYR2* can function redundantly and that their phloem-restricted expression is sufficient to complement the loss-of-function phenotype in the double mutant background.

### MYR1 probably functions as a transcription factor

G2-like family members, such as G2, ZmGLK1, and PHR1, were shown to function as transcription factors by binding DNA and regulating gene expression at the transcription level (Rossini et al., 2001; Rubio et al., 2001). Even though we did not detect NLSs in MYR1-1, -2, and -3 and MYR2-1.1, -1.2, -2.1, and -3.1 by using PredictNLS, MYR1-3-GFP driven by MYR1 promoter or CaMV 35S promoter was observed in the nucleus, suggesting that MYR1-3 contains a nuclear localization signal. By fusing MYR1-3 full-length and truncated proteins to the GAL4 DNA-binding domain and testing their transactivation activity in a yeast strain, we demonstrated that MYR1-3 can regulate gene expression at transcriptional level in yeast and that both the N- and C-termini have transactivation activity. Considering that MYR1 contains a conserved MYB repeat and that one of MYR1 isoforms localizes to the nucleus and can regulate gene expression in yeast, we concluded that MYR1 functions as a transcription factor.

**_MYR1_ and _MYR2_ are partially redundant genes that may regulate lateral shoot outgrowth by modifying auxin levels**

Single mutants for *MYR2* flowered early. In contrast single mutants for *MYR1* did not show any obvious phenotype. *myr1myr2* double mutants grown under continuous light showed a novel phenotype including elongated petioles, semi-erect leaf orientation, and suppression of lateral shoot outgrowth. Considered together these results indicate that MYR1 and MYR2 are partially redundant genes that affect timing and extent of apical and lateral shoot growth and development. These characteristics we observed for the *myr1myr2* double mutant are reminiscent of shade-avoidance responses and *yucca*, a dominant Arabidopsis mutant with elevated levels of free auxin. Considering that auxin signaling interacts with phytochrome, regulating shade-avoidance responses (for review, see Morelli and Ruberti, 2002), and that YUCCA catalyzes a rate-limiting step in tryptophan-dependent auxin biosynthesis (Zhao et al., 2001), we grew *myr1*, *myr2*, *myr1myr2*, and wt in media containing 5-mT, a toxic tryptophan analog. Preliminary results indicated that *myr1myr2* plants are more resistant to the toxic tryptophan analog compared with wt and single mutants. Thus, MYR1 and MYR2 may be involved in the phloem-mediated integration of tryptophan-dependent auxin biosynthesis.

By introducing *MYR1* genomic DNA driven by *MYR2* putative promoter or *MYR2* genomic DNA driven by *MYR1* putative promoter into *myr1myr2* double mutants, we demonstrated that *MYR1* or *MYR2* genomic DNA driven by *MYR2* or *MYR1* promoter, respectively, can rescue the wild type phenotype except earlier flowering phenotype. Preliminary results indicated that *myr1myr2* plants transformed with *MYR1p-gMYR2-MYR1 3'* or *MYR2p-gMYR2-MYR2 3'* biased to wt or *myr1* plants whereas *myr1myr2* plants transformed with *MYR1p-gMYR1-MYR1 3'* or *MYR2p-gMYR1-MYR2 3'* biased to *myr2* plants for the earlier phenotype, indicating that MYR1 and MYR2 are partially redundant for flowering time.

**Alternative splicing occurring within the MYB-related domain and/or coiled-coil sequences in MYR1 and MYR2 may increase their functional diversity**

By screening of the PCR products amplified from the bark cDNA library (Zhao et al., 2000) and/or first cDNA that was reverse transcribed from young seedling and mature plant total

RNA, we isolated 4 isoforms of *MYR1* and 3 isoforms of *MYR2*. SplicePredictor (http://bioinformatics.iastate.edu/cgi-bin/sp.cgi) and/or NetPlantGene (http://www.cbs.dtu.dk/services/NetPGene/) predicted the alternative 3' splicing sites of intron 6 for *MYR1-1* and *MYR1-3*, but not for *MYR1-2*. Since the DNA sequence flanking the alternative 3' splice sites of intron 6 in *MYR1* was highly conserved with that of intron 4 in *MYR2* and SplicePredictor predicted 3 alternative 3' splice sites of intron 4 in *MYR2*, it is likely that *MYR1* has three isoforms generated from alternative 3' splicing of intron 6. To date, three isoforms of *MYR1* generated from alternative 3' splicing of intron 6 have been reported (http://www.arabidopsis.org). We isolated the fourth isoform from the bark library. This isoform included introns 2 to 5 and part of intron 6, but deleted part of exon 7, resulting in a premature stop codon and predicated to produce a truncated protein. It is fairly common for plants to produce transcripts that contain unspliced introns (Lorkovic et al., 2000). The predicted truncated MYR1-4 protein contains less than half of the MYB-related domain. It is not clear whether *MYR1-4* is an inefficiently spliced isoform or has biological significance. Since the splice sites in this isoform are not conserved (Lorkovic et al., 2000), i.e., they can not be predicted by software such as SplicePredicator and NetPlantGene, and several independent RT-PCR experiments did not amplified this isoform from young tissues (data not shown), it is possible that this isoform was produced by defects of the spliceosome in old phloem.

SplicePredictor predicted 3 alternative 3' splice sites for intron 4 and 2 alternative 3' splice sites for intron 1 in *MYR2*. We isolated three isoforms generated from alternative 3' splicing of intron 4, which share the same alternative 3' splicing site of intron 1 (we named them *MYR2-1.1*, *-2.1*, and *-3.1*). The fourth isoform (we named it *MYR2-1.2*) has been reported (www.arabidopsis.org). *MYR2.-1.1* and *-1.2* were generated from alternative 3' splicing of intron 1 and share the same alternative 3' splice site of intron 4. Although we have isolated only 3 isoforms, it is likely that MYR2 has 6 isoforms.

We noted that the alternative splice sites in *MYR1* and *MYR2* are located in the MYB-related domain and/or the coiled-coil regions and amino acid variations induced by alternative splicing does not disrupt the MYB-related domain and/or the coiled-coil regions

at least based on the predictions by Pfam and COILS, respectively. Large-scale computational investigations showed that up to 28% of alternative splicing occurs within annotated domains or functional elements even though it is less than expected by chance, and this kind of alternative splicing frequently inserts or deletes functional residues to modulate function of protein domains/motifs (Kriventseva et al., 2003). Structural variations induced by alternative splicing within the DNA binding domain or the coiled-coil regions may allow a transcription factor to bind target sequences with different affinities or specificities by forming distinct homodimers or heterodimer complexes with relevance to different developmental stages and in the face of different environmental cues (for review, see Lopez, 1995). It is not yet known whether MYR1 and MYR2 bind to their target sequences as homodimers or heterodimers, and whether splicing of *MYR1* and *MYR2* is developmentally regulated. For some transformants, overexpression of *MYR1-1*, *-2*, and *-3*, *MYR2-1.1*, *-2.1*, and *-3.1* driven by the 35S promoter resulted in the same phenotype observed in the *myr1myr2* double mutant, suggesting that MYR1 and MYR2 bind to their target sequences as heterodimers and that overexpression of any one of *MYR1* or *MYR2* isoforms can disrupt, i.e., poison, the activity that depends on formation of specific dimer combinations.

Many questions regarding *MYR1* and *MYR2* remain to be answered, such as, how does *MYR1* and *MYR2* expression become activated? What kind of spliceosome regulates the alternative splicing? How do environmental or developmental or organ-specific cues affect the regulation? Do MYR1 and MYR2 function in auxin-, light-dependent, or other pathway? Which pair of isoforms is functional if MYR1 and/or MYR2 bind to their target sequences as heterodimers? What are downstream direct targets of MYR1 and/or MYR2?

## References

Beveridge CA, Ross JJ, Murfet IC. 1996. Branching in Pea (Action of Genes Rms3 and Rms4). Plant Physiol. 110: 859-865.

Beveridge CA, Symons GM, Turnbull CG. 2000. Auxin inhibition of decapitation-induced branching is dependent on graft-transmissible signals regulated by genes Rms1 and Rms2. Plant Physiol. 123: 689-98.

Booker J, Auldridge M, Wills S, McCarty D, Klee H, Leyser O. 2004. MAX3/CCD7 is a carotenoid cleavage dioxygenase required for the synthesis of a novel plant signaling molecule. Curr Biol. 14:1232-8.

Booker J, Sieberer T, Wright W, Williamson L, Willett B, Stirnberg P, Turnbull C, Srinivasan M, Goddard P, Leyser O. 2005. MAX1 encodes a cytochrome P450 family member that acts downstream of MAX3/4 to produce a carotenoid-derived branch-inhibiting hormone. Dev Cell. 8: 443-9.

Brinkman FSL, Leipe DD. 2001. Phylogenetic analysis. In: Bioinformatics: a practical guide to the analysis of genes and proteins (ed. Baxevanis AD, Ouellette BFF), pp. 323-358. Wiley-InterScience, New York.

Bonke M, Thitamadee S, Mahonen AP, Hauser MT, Helariutta Y. 2003. APL regulates vascular tissue identity in Arabidopsis. Nature. 426: 181-6.

Chen S, Glawischnig E, Jorgensen K, Naur P, Jorgensen B, Olsen CE, Hansen CH, Rasmussen H, Pickett JA, Halkier BA. 2003. CYP79F1 and CYP79F2 have distinct functions in the biosynthesis of aliphatic glucosinolates in Arabidopsis. Plant J. 33: 923-37.

Chisholm ST, Parra MA, Anderberg RJ, Carrington JC. 2001. Arabidopsis RTM1 and RTM2 genes function in phloem to restrict long-distance movement of tobacco etch virus. Plant Physiol.127: 1667-75.

del Pozo JC, Dharmasiri S, Hellmann H, Walker L, Gray WM, Estelle M. 2002. AXR1-ECR1-dependent conjugation of RUB1 to the Arabidopsis Cullin AtCUL1 is required for auxin response. Plant Cell.14: 421-33.

Devlin PF, Yanovsky MJ, Kay SA. 2003. A genomic analysis of the shade avoidance response in Arabidopsis. Plant Physiol. 133: 1617-29.

Doebley J, Stec A, Hubbard L. 1997. The evolution of apical dominance in maize. Nature. 386: 485-8.

Emery JF, Floyd SK, Alvarez J, Eshed Y, Hawker NP, Izhaki A, Baum SF, Bowman JL. 2003. Radial patterning of Arabidopsis shoots by class III HD-ZIP and KANADI genes. Curr Biol. 13: 1768-74.

Evans MM, Barton MK. 1997. Genetics of angiosperm shoot apical meristem development. Annu Rev Plant Physiol Plant Mol Biol. 48: 673-701.

Fitter DW, Martin DJ, Copley MJ, Scotland RW, Langdale JA. 2002. GLK gene pairs regulate chloroplast development in diverse plant species. Plant J. 31: 713-27.

Foo E, Bullier E, Goussot M, Foucher F, Rameau C, Beveridge CA. 2005. The Branching Gene RAMOSUS1 Mediates Interactions among Two Novel Signals and Auxin in Pea. Plant Cell. 17: 464-74.

Foo E, Turnbull CG, Beveridge CA. 2001. Long-distance signaling and the control of branching in the rms1 mutant of pea. Plant Physiol. 126: 203-9.

Gallavotti A, Zhao Q, Kyozuka J, Meeley RB, Ritter MK, Doebley JF, Pe ME, Schmidt RJ. 2004. The role of barren stalk1 in the architecture of maize. Nature. 432: 630-5.

Greb T, Clarenz O, Schafer E, Muller D, Herrero R, Schmitz G, Theres K. 2003. Molecular analysis of the LATERAL SUPPRESSOR gene in Arabidopsis reveals a conserved control mechanism for axillary meristem formation. Genes Dev. 17: 1175-87.

Hall LN, Rossini L, Cribb L, Langdale JA. 1998. GOLDEN 2: a novel transcriptional regulator of cellular differentiation in the maize leaf. Plant Cell. 10: 925-36.

Hansen CH, Wittstock U, Olsen CE, Hick AJ, Pickett JA, Halkier BA. 2001. Cytochrome p450 CYP79F1 from arabidopsis catalyzes the conversion of dihomomethionine and trihomomethionine to the corresponding aldoximes in the biosynthesis of aliphatic glucosinolates. J Biol Chem. 276:11078-85.

Howell SH, Lall S, Che P. 2003. Cytokinins and shoot development. Trends Plant Sci. 8: 453-9.

Ishikawa S, Maekawa M, Arite T, Onishi K, Takamure I, Kyozuka J. 2005. Suppression of tiller bud activity in tillering dwarf mutants of rice. Plant Cell Physiol. 46:79-86.

Kerstetter RA, Bollman K, Taylor RA, Bomblies K, Poethig RS. 2001. KANADI regulates organ polarity in Arabidopsis. Nature. 411: 706-9.

Komatsu K, Maekawa M, Ujiie S, Satake Y, Furutani I, Okamoto H, Shimamoto K, Kyozuka J. 2003. LAX and SPA: major regulators of shoot branching in rice. Proc Natl Acad Sci U S A. 100: 11765-70.
Kriventseva EV, Koch I, Apweiler R, Vingron M, Bork P, Gelfand MS, Sunyaev S. 2003. Increase of functional diversity by alternative splicing. Trends Genet. 19: 124-8.
Leyser O. 2003. Regulation of shoot branching by auxin. Trends Plant Sci. 8: 541-5.
Leyser HM, Lincoln CA, Timpte C, Lammer D, Turner J, Estelle M. 1993. Arabidopsis auxin-resistance gene AXR1 encodes a protein related to ubiquitin-activating enzyme E1. Nature. 364: 161-4.
Leyser HM, Pickett FB, Dharmasiri S, Estelle M. 1996. Mutations in the AXR3 gene of Arabidopsis result in altered auxin response including ectopic expression from the SAUR-AC1 promoter. Plant J. 10: 403-13.
Li X, Qian Q, Fu Z, Wang Y, Xiong G, Zeng D, Wang X, Liu X, Teng S, Hiroshi F, Yuan M, Luo D, Han B, Li J. 2003. Control of tillering in rice. Nature. 422: 618-21.
Lopez AJ. 1995. Developmental role of transcription factor isoforms generated by alternative splicing. Dev Biol. 172: 396-411.
Lorkovic ZJ, Wieczorek Kirk DA, Lambermon MH, Filipowicz W. 2000. Pre-mRNA splicing in higher plants. Trends Plant Sci. 5:160-7.
Morelli G, Ruberti I. 2002. Light and shade in the photocontrol of Arabidopsis growth. Trends Plant Sci.7: 399-404.
Morris SE, Turnbull CG, Murfet IC, Beveridge CA. 2001. Mutational analysis of branching in pea. Evidence that Rms1 and Rms5 regulate the same novel signal. Plant Physiol. 126: 1205-13.
Napoli C. 1996. Highly Branched Phenotype of the Petunia dad1-1 Mutant Is Reversed by Grafting. Plant Physiol. 111: 27-37.
Napoli CA, Beveridge CA, Snowden KC. 1999. Reevaluating concepts of apical dominance and the control of axillary bud outgrowth. Curr Top Dev Biol. 44: 127-69.
Neter J, Kutner MH, Nachtsheim CJ, Wasserman W. 1996. Applied linear statistical models. The McGraw-Hill Companies, Inc..
Nordstrom A, Tarkowski P, Tarkowska D, Norbaek R, Astot C, Dolezal K, Sandberg G. 2004. Auxin regulation of cytokinin biosynthesis in Arabidopsis thaliana: a factor of

potential importance for auxin-cytokinin-regulated development. Proc Natl Acad Sci U S A. 101: 8039-44.
Ouellet F, Overvoorde PJ, Theologis A. 2001. IAA17/AXR3: biochemical insight into an auxin mutant phenotype. Plant Cell.13: 829-41.
Rameau C, Murfet IC, Laucou V, Floyd RS, Morris SE, Beveridge CA. 2002. Pea rms6 mutants exhibit increased basal branching. Physiol Plant. 115: 458-467.
Riechmann JL, Heard J, Martin G, Reuber L, Jiang C, Keddie J, Adam L, Pineda O, Ratcliffe OJ, Samaha RR, Creelman R, Pilgrim M, Broun P, Zhang JZ, Ghandehari D, Sherman BK, Yu G. 2000. Arabidopsis transcription factors: genome-wide comparative analysis among eukaryotes. Science. 290: 2105-10.
Rogg LE, Lasswell J, Bartel B. 2001. A gain-of-function mutation in IAA28 suppresses lateral root development. Plant Cell. 13: 465-80.
Rossini L, Cribb L, Martin DJ, Langdale JA. 2001. The maize golden2 gene defines a novel class of transcriptional regulators in plants. Plant Cell. 13: 1231-44.
Rubio V, Linhares F, Solano R, Martin AC, Iglesias J, Leyva A, Paz-Ares J. 2001. A conserved MYB transcription factor involved in phosphate starvation signaling both in vascular plants and in unicellular algae. Genes Dev. 15: 2122-33.
Sakai H, Aoyama T, Bono H, Oka A. 1998. Two-component response regulators from Arabidopsis thaliana contain a putative DNA-binding motif. Plant Cell Physiol. 39: 1232-9.
Schmitz G, Tillmann E, Carriero F, Fiore C, Cellini F, Theres K. 2002. The tomato Blind gene encodes a MYB transcription factor that controls the formation of lateral meristems. Proc Natl Acad Sci U S A. 99: 1064-9.
Schumacher K, Schmitt T, Rossberg M, Schmitz G, Theres K. 1999. The Lateral suppressor (Ls) gene of tomato encodes a new member of the VHIID protein family. Proc Natl Acad Sci U S A. 96: 290-5.
Shimizu-Sato S, Mori H. 2001. Control of outgrowth and dormancy in axillary buds. Plant Physiol. 127: 1405-13.
Snowden KC and Napoli C. 2003. A quantitative study and lateral branching in petunia. Funct. Plant Biol. 30: 987-994.
Snowden KC, Simkin AJ, Janssen BJ, Templeton KR, Loucas HM, Simons JL, Karunairetnam S, Gleave AP, Clark DG, Klee HJ. 2005. The Decreased apical

dominance1/Petunia hybrida CAROTENOID CLEAVAGE DIOXYGENASE8 Gene Affects Branch Production and Plays a Role in Leaf Senescence, Root Growth, and Flower Development. Plant Cell. 17: 746-59.
Sorefan K, Booker J, Haurogne K, Goussot M, Bainbridge K, Foo E, Chatfield S, Ward S, Beveridge C, Rameau C, Leyser O. 2003. MAX4 and RMS1 are orthologous dioxygenase-like genes that regulate shoot branching in Arabidopsis and pea. Genes Dev. 17: 1469-74.
Stirnberg P, Chatfield SP, Leyser HM. 1999. AXR1 acts after lateral bud formation to inhibit lateral bud growth in Arabidopsis. Plant Physiol.121: 839-47.
Stirnberg P, van De Sande K, Leyser HM. 2002. MAX1 and MAX2 control shoot lateral branching in Arabidopsis. Development. 129: 1131-41.
Stracke R, Werber M, Weisshaar B. 2001. The R2R3-MYB gene family in Arabidopsis thaliana. Curr Opin Plant Biol. 4: 447-56.
Takeda T, Suwa Y, Suzuki M, Kitano H, Ueguchi-Tanaka M, Ashikari M, Matsuoka M, Ueguchi C. 2003. The OsTB1 gene negatively regulates lateral branching in rice. Plant J. 33: 513-20.
Talbert PB, Adler HT, Parks DW, Comai L. 1995. The REVOLUTA gene is necessary for apical meristem development and for limiting cell divisions in the leaves and stems of Arabidopsis thaliana. Development.121: 2723-35.
Tantikanjana T, Yong JW, Letham DS, Griffith M, Hussain M, Ljung K, Sandberg G, Sundaresan V. 2001. Control of axillary bud initiation and shoot architecture in Arabidopsis through the SUPERSHOOT gene. Genes Dev. 15: 1577-88.
Tantikanjana T, Mikkelsen MD, Hussain M, Halkier BA, Sundaresan V. 2004. Functional analysis of the tandem-duplicated P450 genes SPS/BUS/CYP79F1 and CYP79F2 in glucosinolate biosynthesis and plant development by Ds transposition-generated double mutants. Plant Physiol. 135: 840-8.
Thelander M, Fredriksson D, Schouten J, Hoge JH, Ronne H. 2002. Cloning by pathway activation in yeast: identification of an Arabidopsis thaliana F-box protein that can turn on glucose repression. Plant Mol Biol. 49: 69-79.
Ward SP, Leyser O. 2004. Shoot branching. Curr Opin Plant Biol. 7: 73-8.

Wykoff DD, Grossman AR, Weeks DP, Usuda H, Shimogawara K. 1999. Psr1, a nuclear localized protein that regulates phosphorus metabolism in Chlamydomonas. Proc Natl Acad Sci U S A. 96: 15336-41.

Zhao C, Johnson BJ, Kositsup B, Beers EP. 2000. Exploiting secondary growth in Arabidopsis. Construction of xylem and bark cDNA libraries and cloning of three xylem endopeptidases. Plant Physiol. 123: 1185-96.

Zhao C, Craig JC, Petzold HE, Dickerman AW, Beers EP. 2005. The xylem and phloem transcriptomes from secondary tissues of the Arabidopsis root-hypocotyl. Plant Physiol. 138. in press.

Zhao Y, Christensen SK, Fankhauser C, Cashman JR, Cohen JD, Weigel D, Chory J. 2001. A role for flavin monooxygenase-like enzymes in auxin biosynthesis. Science. 291: 306-9.

Zhong R, Ye ZH. 2001. Alteration of auxin polar transport in the Arabidopsis ifl1 mutants. Plant Physiol.126: 549-63.

Zubko E, Adams CJ, Machaekova I, Malbeck J, Scollan C, Meyer P. 2002. Activation tagging identifies a gene from Petunia hybrida responsible for the production of active cytokinins in plants. Plant J. 29: 797-808.